Double obstacle phase field approach to an inverse problem for a discontinuous diffusion coefficient

Article (Accepted Version)

Double obstacle phase field approach to an inverse problem for a discontinuous diffusion coefficient

Klaus Deckelnick[*], Charles M. Elliott[†] and Vanessa Styles[‡]

Abstract

We propose a double obstacle phase field approach to the recovery of piece-wise constant diffusion coefficients for elliptic partial differential equations. The approach to this inverse problem is that of optimal control in which we have a quadratic fidelity term to which we add a perimeter regularisation weighted by a parameter σ. This yields a functional which is optimised over a set of diffusion coefficients subject to a state equation which is the underlying elliptic PDE. In order to derive a problem which is amenable to computation the perimeter functional is relaxed using a gradient energy functional together with an obstacle potential in which there is an interface parameter ϵ. This phase field approach is justified by proving $\Gamma-$convergence to the functional with perimeter regularisation as $\epsilon \to 0$. The computational approach is based on a finite element approximation. This discretisation is shown to converge in an appropriate way to the solution of the phase field problem. We derive an iterative method which is shown to yield an energy decreasing sequence converging to a discrete critical point. The efficacy of the approach is illustrated with numerical experiments.

1 Introduction

Many applications lead to mathematical models involving elliptic equations with piece-wise constant discontinuous coefficients. Frequently the interfaces across which the coefficients jump are completely unknown. A common approach for the identification of these coefficients is to make observations of the field variables solving the equations and use these values in an attempt to determine the coefficients by formulating an inverse problem for the coefficients. This is generally ill posed and in applications it is usual to use a fidelity to the observations functional together with a regularisation of the coefficients. In this paper we use a regularisation of the coefficients by employing the perimeter of the jump sets of the coefficients.

[*]Institut für Analysis und Numerik, Otto-von-Guericke-Universität Magdeburg, Universitätsplatz 2, 39106 Magdeburg, Germany.

[†]Mathematics Institute, University of Warwick, Coventry CV4 7AL, UK.

[‡]Department of Mathematics, University of Sussex, Brighton BN1 9RF, UK.

1.1 Model problem

To fix ideas we consider the following model elliptic problem:

$$-\nabla \cdot \big(a \nabla y\big) = 0 \quad \text{in } \Omega \tag{1.1}$$

$$a \frac{\partial y}{\partial \nu} = g \quad \text{on } \partial\Omega, \tag{1.2}$$

where Ω is a bounded domain in $\mathbb{R}^d$ $(d = 2, 3)$, g is given boundary data with zero mean

$$\int_{\partial\Omega} g = 0 \tag{1.3}$$

and a is an isotropic diffusion (conductivity) coefficient. We suppose that the diffusion coefficient takes one of the r positive values $a_1, \ldots, a_r$. Our interest is in modelling a geometrical inverse problem concerning the determination of the regions in which the material diffusion coefficient takes these values. Our problem then is to determine the sets $E_i = \{x \in \Omega \,|\, a(x) = a_i\}$ given observations of the solution y of the elliptic boundary value problem (1.1), (1.2). In the case of $r = 2$, under constraints on the nature of the domains and boundary conditions, uniqueness and stability results have been proved in [7, 2]. In this context see also [28].
A standard approach is to minimise a fidelity functional

$$J_{fid}(\mathcal{E}) := ||y_{\mathcal{E}} - y_{obs}||^2_{\mathcal{O}}$$

over an appropriate class of partitions $\mathcal{E} = (E_i)_{i=1}^r$ of Ω, where $y_{\mathcal{E}}$ denotes the solution of the state or forward equation (1.1), (1.2) with diffusion coefficient $a(x) = a_i, x \in E_i, i = 1, \ldots, r$. Furthermore, $\mathcal{O}$ is an appropriate space of observations and $y_{obs} \in \mathcal{O}$ is given. In general this problem is ill-posed and is typically regularised by adding a Tikhonov regularisation functional. A numerical approach without regularisation is proposed in [28, 32].

1.2 Geometric regularisation

In this setting it has been considered appropriate to use perimeter regularisation, [34, 31]

$$J_{reg}(\mathcal{E}) = \hat{\sigma} \sum_{i=1}^{r} \mathcal{H}^{d-1}(\partial E_i \cap \Omega), \quad \mathcal{E} = (E_i)_{i=1}^r,$$

where the regularisation parameter $\hat{\sigma}$ is positive. Minimisers of

$$J(\mathcal{E}) := J_{fid}(\mathcal{E}) + J_{reg}(\mathcal{E})$$

are then typically sought in the set of Caccioppoli partitions into r components, i.e. partitions $\mathcal{E} = (E_i)_{i=1}^r$ of Ω with $\mathcal{H}^d(E_i \cap E_j) = 0, i \neq j$, $\mathcal{H}^d\big(\Omega \setminus \bigcup_{i=1}^r E_i\big) = 0$ for which $u_i := \chi_{E_i}$ belongs to $BV(\Omega), i = 1, \ldots, r$. Thus, a Caccioppoli partition corresponds to a function $\mathbf{u} = (u_1, \ldots, u_r) \in BV(\Omega, \{e_1, \ldots, e_r\})$, where $e_1, \ldots, e_r$ are the unit vectors in $\mathbb{R}^r$. We can then write the regularisation functional in terms of $\mathbf{u}$ as follows:

$$J_{reg}(\mathbf{u}) = \hat{\sigma} \sum_{i=1}^{r} \int_{\Omega} |Du_i|.$$

Here, $\int_\Omega |Du_i|$ is the total variation of the vector–valued Radon measure Du_i. Before we rewrite the fidelity term let us introduce the Gibbs simplex

$$\Sigma := \{\mathbf{y} \in \mathbb{R}^r \,|\, y_i \geq 0, i = 1, \ldots, r, \; \sum_{i=1}^r y_i = 1\}$$

and observe that $e_1, \ldots, e_r$ are the corners of Σ. Consider the set

$$X := \{\mathbf{u} : \Omega \to \mathbb{R}^r \,|\, \mathbf{u} \text{ is measurable and } \mathbf{u}(x) \in \Sigma \text{ a.e. in } \Omega\}$$

endowed with the L^1–norm and define for $\mathbf{u} \in X$

$$a(\mathbf{u}) := \sum_{i=1}^r a_i u_i \tag{1.4}$$

and by $S(\mathbf{u})$ the solution of (1.1), (1.2) with diffusion coefficient $a(\mathbf{u})$.
We set $\hat{\sigma} = \frac{\pi}{8}\sigma$ for later convenience. The constant $\pi/8$ arises from the form of the phase field relaxation used in (1.5), see (2.7).
Problem (**PGR**) is then to seek minimizers of the functional $J : X \to \mathbb{R} \cup \{\infty\}$ given by

$$J(\mathbf{u}) := \begin{cases} \frac{1}{2}||S(\mathbf{u}) - y_{obs}||^2_{\mathcal{O}} + \sigma\frac{\pi}{8}\sum_{i=1}^r \int_\Omega |Du_i| & , \text{ if } \mathbf{u} \in BV(\Omega, \{e_1, \ldots, e_r\}) \cap X; \\ \infty & , \text{ otherwise.} \end{cases}$$

In this problem the fidelity term is non-convex because of the nonlinearity of the state solution operator $S(\cdot)$ with respect to the coefficient $a(\mathbf{u})$. Also a feature of this natural geometric regularisation approach is that the regularisation functional is non-convex. This is reflected in the fact that $\mathbf{u}$ only takes one of the values $e_1, \ldots, e_r$ which leads to a non–convex constraint.

1.3 Double obstacle phase field approach

We shall consider a suitable phase field approximation of the above regularisation which involves gradient energies and functions that map into the Gibbs simplex. In this approximation we relax the non-convex constraint $\mathbf{u}(x) \in \{e_1, \ldots, e_r\}$ by introducing the set

$$\mathcal{K} := \{\mathbf{u} \in H^1(\Omega, \mathbb{R}^r) \,|\, \mathbf{u}(x) \in \Sigma \text{ a.e. in } \Omega\}$$

and approximate J by the sequence of functionals $J_\epsilon : X \to \mathbb{R} \cup \{\infty\}, \epsilon > 0$ with

$$J_\epsilon(\mathbf{u}) := \begin{cases} \frac{1}{2}||S(\mathbf{u}) - y_{obs}||^2_{\mathcal{O}} + \sigma \int_\Omega \big(\frac{\varepsilon}{2}|D\mathbf{u}|^2 + \frac{1}{2\varepsilon}(1 - |\mathbf{u}|^2)\big)dx & , \text{ if } \mathbf{u} \in \mathcal{K}; \\ \infty & , \text{ otherwise.} \end{cases} \tag{1.5}$$

Here, $\int_\Omega |D\mathbf{u}|^2 dx = \sum_{i=1}^r \int_\Omega |\nabla u_i|^2 dx$ and for $\mathbf{u} \in \mathcal{K}$ we have $\int_\Omega (1 - |\mathbf{u}|^2) = \sum_{i=1}^r \int_\Omega u_i(1 - u_i)$. Problem (**PDO**) is then to seek minimisers of J_ε. We refer to this approach as a double obstacle phase field model because of the constraints $0 \leq u_i \leq 1$ on the components of the phase field vector $\mathbf{u}$. The parameter ϵ is a measure of the thickness of a diffuse interface

separating two sets on which the diffusion coefficient is constant. The Cahn–Hilliard type energy

$$\int_\Omega \big(\frac{\varepsilon}{2}|\nabla u|^2 + \frac{1}{2\varepsilon}(u-u^2)\big)dx$$

is well established as an approximation of the perimeter functional, see e.g. [12, 11, 6]. Note that the regularisation remains non-convex through the quadratic Cahn-Hilliard functional even though the constraint set is convex. Let us remark that such a phase field model has recently been used in a binary recovery problem, see [15].

Note that we view (**PGO**) as having just one regularisation parameter σ. The ε parameter in (**PGO**) may be viewed as a way of providing an approximation of (**PGR**) which is computationally accessible.

1.4 Other approaches

There have been attempts to solve the recovery problem without regularisation of the interfaces across which the diffusion coefficients jump. Formally one can write down variations of the fidelity functional with respect to variations of the interfaces. For example see [28]. In particular the interfaces can be associated with particular level sets of level set functions which have to be determined. We refer to [36, 32, 24, 16] for numerical implementations. The use of level set descriptions of the interfaces in the context of perimeter regularisations is described in [3, 26, 27]. Related to this is the use of total variation of a regularised Heaviside function with argument being a level set function, [22, 40]. In [19] the authors consider the distributed control of linear elliptic systems in which the control variable should only take on a finite number of values. To this purpose they introduce a combination of L^2 and L^0–type penalties whose Fenchel conjugates allow the derivation of a primal–dual optimality system with a unique solution. A suitable adaption of this approach could be an alternative way to attack the inverse problem considered in the present paper.
In the different context of image segmentation parametric description of curves have been used in conjunction with perimeter regularisation, [8, 39].
On the other hand [17, 38, 35] use total variation regularisation and relax the constraints that the indicator functions take just two values.

1.5 Applications

Our model problem is an example of the identification of a coefficient in an elliptic equation. This problem arises in many applications. For example, a fundamental issue in the use of mathematical models of flow in porous media is that the geological features which determine the permeability are unknown. In geology a facies is a body of rock with specific characteristics. In our model problem y is the pressure or hydraulic head associated with a fluid (for example, oil or water) occupying the reservoir or acquifer Ω and a is the permeability of the rock. We assume that the permeability is isotropic and is piece-wise constant. The domains $E_i = \{x \in \Omega \,|\, a(x) = a_i\},\ i = 1, 2, ..., r$ model the decomposition of the reservoir Ω into facies whose location is unknown. The goal is to use observations of the pressure to determine the geometrical decomposition of the reservoir with respect to these facies, [25, 30, 29].

Such problems also arise in imaging. For example, electric impedance tomography, [18, 24, 13], is the determination of the conductivity distribution in the interior of a domain using observations of current and potential. Here y is the electric potential and a is a conductivity which takes different values in unknown interior domains. In medical imaging the shape and size of interior domains may be inferred from the variation of the conductivity.

1.6 Outline and contributions of the paper

- In Section 2 we introduce the functionals J_ϵ and prove that they Γ–converge to J. Furthermore, we show that J_ϵ has a minimum and derive a necessary first order condition. This establishes that problems (**PGR**) and (**PDO**) have solutions.
- The optimisation problem in Section 2 is infinite-dimensional. In order to carry out numerical calculations we employ a finite element spatial discretisation. This is derived in Section 3 and we prove convergence results for absolute minimizers and critical points as the mesh size tends to zero. This establishes that the inverse problems (**PGR**) and (**PDO**) can be approximated by something computable.
- Section 4 is devoted to formulating an iterative scheme for finding critical points of the functional associated with the discrete optimisation problem. The method is based on a semi-implicit time discretisation of a parabolic variational inequality which is a gradient flow for the energy. In this finite dimensional setting we prove a global convergence result for the iteration.
- Finally in Section 5 we illustrate the applicability of the method with some numerical examples.

2 Problem formulation

2.1 State equation

Let $\Omega \subset \mathbb{R}^d$ be a bounded domain with a Lipschitz boundary. We suppose that $g \in L^2(\partial\Omega)$ satisfying (1.3) and $y_{obs} \in \mathcal{O}$ are given functions. Here, $\big(\mathcal{O}, (\cdot,\cdot)_{\mathcal{O}}\big)$ is a Hilbert space with the property that $H^1(\Omega)$ is compactly embedded in $\mathcal{O}$. Furthermore we assume that the following Poincaré inequality

$$||\eta - \mathcal{M}_{\mathcal{O}}(\eta)|| \leq C_p||\nabla\eta||, \qquad \eta \in H^1(\Omega) \tag{2.1}$$

holds, where $||\cdot||$ denotes the $L^2(\Omega)$ norm and $\mathcal{M}_{\mathcal{O}}(\eta)$ denotes the mean value of η with

$$\mathcal{M}_{\mathcal{O}}(\eta) := (\eta, 1)_{\mathcal{O}}/||1||^2_{\mathcal{O}}, \quad \eta \in \mathcal{O}.$$

Typical examples are $\mathcal{O} = L^2(\Omega)$ or $L^2(\partial\Omega)$ representing either bulk measurements or boundary observations of the solution of the state equation.
For a given $\mathbf{u} \in X$ we denote by $y = S(\mathbf{u}) \in H^1(\Omega)$ the unique weak solution of the Neumann problem

$$-\nabla \cdot (a(\mathbf{u})\nabla y) = 0 \quad \text{in } \Omega \tag{2.2}$$

$$a(\mathbf{u})\frac{\partial y}{\partial \nu} = g \quad \text{on } \partial\Omega \tag{2.3}$$

with $\mathcal{M}_{\mathcal{O}}(y) = \mathcal{M}_{\mathcal{O}}(y_{obs})$ in the sense that

$$\int_\Omega a(\mathbf{u})\nabla y \cdot \nabla \eta dx = \int_{\partial\Omega} g\eta do \qquad \forall \eta \in H^1(\Omega). \tag{2.4}$$

Here, $a(\mathbf{u})$ is given by (1.4), where we note that

$$a_{min} \leq a(\mathbf{u}) \leq a_{max} \quad \text{ a.e. in } \Omega, \text{ uniformly in } \mathbf{u} \in X, \tag{2.5}$$

where $a_{min} := \min(a_1, \ldots, a_r)$, $a_{max} := \max(a_1, \ldots, a_r)$. Observe that S is a nonlinear operator because of the bilinear relation between $a(\mathbf{u})$ and y in (2.4). Using (2.1) together with the fact that $\mathcal{M}_{\mathcal{O}}(y) = \mathcal{M}_{\mathcal{O}}(y_{obs})$ we infer that the solution $y = S(\mathbf{u})$ satisfies

$$\|y\| \leq \|y - \mathcal{M}_{\mathcal{O}}(y)\| + |\Omega|^{\frac{1}{2}}|\mathcal{M}_{\mathcal{O}}(y_{obs})| \leq C_p\|\nabla y\| + \frac{|\Omega|^{\frac{1}{2}}}{||1||_{\mathcal{O}}}\|y_{obs}\|_{\mathcal{O}}.$$

If we combine this estimate with the choice $\eta = y$ in (2.4) and use (2.5) as well as the continuous embedding $H^1(\Omega) \hookrightarrow L^2(\partial\Omega)$ we deduce that

$$\|S(\mathbf{u})\|_{H^1(\Omega)} \leq c(a_{min}, \Omega)\big(\|g\|_{L^2(\partial\Omega)} + \|y_{obs}\|_{\mathcal{O}}\big) \quad \text{ uniformly in } \mathbf{u} \in X. \tag{2.6}$$

We see that the problem of observing y given $\mathbf{u}$ is well formulated because

$$S : X \to \mathcal{O} \quad \text{is continuous}$$

which is a consequence of the following lemma.

Lemma 2.1. *$S : X \to H^1(\Omega)$ is continuous.*

Proof. Let $\mathbf{u} \in X$ and $(\mathbf{u}_k)_{k\in\mathbb{N}}$ a sequence in X with $\mathbf{u}_k \to \mathbf{u}$ in $L^1(\Omega, \mathbb{R}^r), k \to \infty$. Since $0 \leq u_{k,i} \leq 1, i = 1, \ldots, r$ we may assume by passing to a subsequence if necessary that $\mathbf{u}_k \to \mathbf{u}$ in $L^2(\Omega, \mathbb{R}^r)$ and a.e. in Ω. Abbreviating $y = S(\mathbf{u}), y_k = S(\mathbf{u}_k)$ we have for $\eta \in H^1(\Omega)$

$$\int_\Omega a(\mathbf{u}_k)\nabla(y_k - y) \cdot \nabla\eta dx = \int_\Omega (a(\mathbf{u}) - a(\mathbf{u}_k))\nabla y \cdot \nabla\eta dx.$$

Choosing $\eta = y_k - y$ we deduce with the help of (2.5) and (1.4)

$$a_{min}\|\nabla(y_k - y)\| \leq a_{max}\Big(\int_\Omega |\mathbf{u}_k - \mathbf{u}|^2|\nabla y|^2 dx\Big)^{\frac{1}{2}} \to 0, k \to \infty$$

by the dominated convergence theorem because

$$|\mathbf{u}_k - \mathbf{u}|^2|\nabla y|^2 \to 0 \text{ a.e. in } \Omega, \quad |\mathbf{u}_k - \mathbf{u}|^2|\nabla y|^2 \leq r|\nabla y|^2 \text{ a.e in } \Omega \text{ and } |\nabla y|^2 \in L^1(\Omega).$$

Since $\mathcal{M}_{\mathcal{O}}(y_k - y) = 0$ we deduce with the help of (2.1) that $S(\mathbf{u}_k) = y_k \to y = S(\mathbf{u})$ in $H^1(\Omega)$. □

2.2 Γ–convergence and existence of minimizers

The use of J_ϵ in the minimization of J is justified by the following Γ–convergence result.

Theorem 2.2. *The functionals J_ϵ Γ–converge to J in X.*

Proof. Let us write $J_\epsilon(\mathbf{u}) = G(\mathbf{u}) + \sigma F_\epsilon(\mathbf{u})$, where $G(\mathbf{u}) = \frac{1}{2}||S(\mathbf{u}) - y_{obs}||^2_{\mathcal{O}}$ is continuous as a consequence of Lemma 2.1 and the embedding of $H^1(\Omega)$ into $\mathcal{O}$. In Theorem 6.1 in the Appendix we show that

$$F_\epsilon \xrightarrow{\Gamma} F, \text{ where } F(\mathbf{u}) = \begin{cases} \frac{\pi}{8}\sum_{i=1}^{r}\int_\Omega |Du_i| & , \text{ if } \mathbf{u} \in BV(\Omega, \{e_1, \dots, e_r\}) \cap X; \\ \infty & , \text{ otherwise.} \end{cases} \tag{2.7}$$

Using Remark 1.7 in [14] we infer that $J_\epsilon \xrightarrow{\Gamma} G + \sigma F = J$. □

Theorem 2.3. *The minimization problem $\min_{\mathbf{v}\in X} J_\epsilon(\mathbf{v})$ has a solution $\mathbf{u}_\epsilon \in \mathcal{K}$.*

Proof. Let $(\mathbf{u}_k)_{k\in\mathbb{N}} \subset \mathcal{K}$ be a minimizing sequence, $J_\epsilon(\mathbf{u}_k) \searrow \inf_{\mathbf{v}\in X} J_\epsilon(\mathbf{v})$. Since $(\mathbf{u}_k)_{k\in\mathbb{N}}$ is bounded in $H^1(\Omega, \mathbb{R}^r)$ there exists a subsequence, again denoted by $(\mathbf{u}_k)_{k\in\mathbb{N}}$, and $\mathbf{u}_\epsilon \in H^1(\Omega, \mathbb{R}^r)$ such that

$$\mathbf{u}_k \rightharpoonup \mathbf{u}_\epsilon \text{ in } H^1(\Omega, \mathbb{R}^r), \quad \mathbf{u}_k \to \mathbf{u}_\epsilon \text{ in } L^2(\Omega, \mathbb{R}^r) \text{ and a.e. in } \Omega.$$

In particular, $\mathbf{u}_\epsilon \in \mathcal{K}$. Lemma 2.1 implies that $S(\mathbf{u}_k) \to S(\mathbf{u}_\epsilon)$ in $\mathcal{O}$ which combined with the weak lower semicontinuity of the H^1-seminorm shows that $\mathbf{u}_\epsilon$ is a minimum of J_ϵ. □

Corollary 2.4. *Let $(u_\epsilon)_{\epsilon>0}$ be a sequence of minimizers of J_ϵ. Then there exists a sequence $\epsilon_k \to 0, k \to \infty$ and $\mathbf{u} \in BV(\Omega; \{e_1, \dots, e_r\}) \cap X$ such that $\mathbf{u}_{\epsilon_k} \to \mathbf{u}$ in $L^1(\Omega, \mathbb{R}^r)$ and $\mathbf{u}$ is a minimum of J.*

Proof. By Corollary 6.2 in the Appendix there exists a sequence $\epsilon_k \to 0, k \to \infty$ and $\mathbf{u} \in BV(\Omega; \{e_1, \dots, e_r\}) \cap X$ such that $\mathbf{u}_{\epsilon_k} \to \mathbf{u}$ in $L^1(\Omega, \mathbb{R}^r)$. It is well–known that the Γ–convergence of J_{ϵ_k} to J implies that $\mathbf{u}$ is a minimum of J. □

2.3 Necessary first order condition for the phase field recovery

In order to derive the necessary first order conditions for a minimum of J_ε we consider $\mathcal{K}$ as a subset of $L^\infty(\Omega, \mathbb{R}^r)$. Similarly as in [9], Section 3, one can prove that the solution operator $S : L^\infty(\Omega, \mathbb{R}^r) \supset \mathcal{K} \to H^1(\Omega)$ is Fréchet differentiable with $\tilde{y} = S'(\mathbf{u})\mathbf{w}, \mathbf{w} \in L^\infty(\Omega, \mathbb{R}^r)$ being given as the solution of

$$\int_\Omega a(\mathbf{u})\nabla\tilde{y} \cdot \nabla\eta dx = -\int_\Omega a(\mathbf{w})\nabla S(\mathbf{u}) \cdot \nabla\eta dx \qquad \forall \eta \in H^1(\Omega) \tag{2.8}$$

with $\mathcal{M}_{\mathcal{O}}(\tilde{y}) = 0$. As a result, J_ε is Fréchet differentiable on $\mathcal{K} \subset L^\infty(\Omega, \mathbb{R}^r) \cap H^1(\Omega, \mathbb{R}^r)$ with

$$J'_\varepsilon(\mathbf{u})\mathbf{w} = \big(S(\mathbf{u}) - y_{obs}, S'(\mathbf{u})\mathbf{w}\big)_{\mathcal{O}} + \sigma\int_\Omega \big(\varepsilon D\mathbf{u} \cdot D\mathbf{w} - \frac{1}{\varepsilon}\mathbf{u} \cdot \mathbf{w}\big)dx \tag{2.9}$$

for $\mathbf{w} \in L^\infty(\Omega, \mathbb{R}^r) \cap H^1(\Omega, \mathbb{R}^r)$. In order to avoid the evaluation of $S'(\mathbf{u})\mathbf{w}$ in (2.9) we work as usual with a dual problem: Find $p \in H^1(\Omega)$ such that $\mathcal{M}_{\mathcal{O}}(p) = 0$ and

$$\int_\Omega a(\mathbf{u})\nabla p \cdot \nabla \eta dx = \big(S(\mathbf{u}) - y_{obs}, \eta\big)_{\mathcal{O}} \quad \forall \eta \in H^1(\Omega), \tag{2.10}$$

where we note that the solvability condition $\big(S(\mathbf{u}) - y_{obs}, 1\big)_{\mathcal{O}} = 0$ is satisfied. As a result we obtain from (2.9), (2.10) and (2.8)

$$\begin{aligned} J'_\varepsilon(\mathbf{u})\mathbf{w} &= \int_\Omega a(\mathbf{u})\nabla p \cdot \nabla [S'(\mathbf{u})\mathbf{w}] dx + \sigma \int_\Omega \big(\varepsilon D\mathbf{u} \cdot D\mathbf{w} - \frac{1}{\varepsilon}\mathbf{u} \cdot \mathbf{w}\big) dx \\ &= -\int_\Omega a(\mathbf{w})\, \nabla S(\mathbf{u}) \cdot \nabla p dx + \sigma \int_\Omega \big(\varepsilon D\mathbf{u} \cdot D\mathbf{w} - \frac{1}{\varepsilon}\mathbf{u} \cdot \mathbf{w}\big) dx. \end{aligned}$$

At a minimum $\mathbf{u}$ of J_ϵ we have $J'_\varepsilon(\mathbf{u})(\mathbf{v}-\mathbf{u}) \geq 0$ for all $\mathbf{v} \in \mathcal{K}$. Since $a(\mathbf{v}-\mathbf{u}) = a(\mathbf{v}) - a(\mathbf{u})$ we therefore define:

Definition 2.5. (**Phase field critical point**) Find $\mathbf{u} \in \mathcal{K}$ such that for all $\mathbf{v} \in \mathcal{K}$

$$\sigma \int_\Omega \big(\varepsilon D\mathbf{u} \cdot D(\mathbf{v}-\mathbf{u}) - \frac{1}{\varepsilon}\mathbf{u} \cdot (\mathbf{v}-\mathbf{u})\big) dx - \int_\Omega (a(\mathbf{v}) - a(\mathbf{u}))\, \nabla S(\mathbf{u}) \cdot \nabla p dx \geq 0. \tag{2.11}$$

Remark 2.6. A natural strategy to construct solutions of (2.11) and hence to find candidates for at least a local minimum of J_ε is to consider the following parabolic obstacle problem: Find $\mathbf{u}(\cdot, t) \in \mathcal{K}, t \geq 0$ such that $\mathbf{u}(\cdot, 0) = \mathbf{u}_0$ and

$$(\mathbf{u}_t, \mathbf{v}-\mathbf{u}) + \sigma \int_\Omega \big(\varepsilon D\mathbf{u} \cdot D(\mathbf{v}-\mathbf{u}) - \frac{1}{\varepsilon}\mathbf{u} \cdot (\mathbf{v}-\mathbf{u})\big) dx - \int_\Omega (a(\mathbf{v}) - a(\mathbf{u}))\, \nabla S(\mathbf{u}) \cdot \nabla p dx \geq 0$$

for all $\mathbf{v} \in \mathcal{K}$ and all $t > 0$. Here, p is the solution of (2.10) for $\mathbf{u}(\cdot, t)$ and $\mathbf{u}_0 \in \mathcal{K}$ is a suitably chosen initial function.

Inserting $\mathbf{v} = \mathbf{u}(\cdot, t - \Delta t)$ into the above relation, dividing by Δt and sending $\Delta t \to 0$ we formally find that

$$\|\mathbf{u}_t\|^2 + J'_\epsilon(\mathbf{u})\mathbf{u}_t \leq 0,$$

so that $\dfrac{d}{dt} J_\epsilon(\mathbf{u}(\cdot, t)) \leq 0$ and the value of the objective funtional decreases during the evolution. If $\lim_{t\to\infty} u(\cdot, t) =: u_\infty$ exists, we expect u_∞ to be a solution of (2.11).

3 Finite element approximation

In what follows we assume that Ω is a polygonal (d=2) or polyhedral (d=3) domain. Let us denote by $(\mathcal{T}_h)_{0<h\leq h_0}$ a regular triangulation of Ω and set

$$V_h = \{\chi \in C^0(\bar{\Omega}) \,|\, \chi_{|T} \in P_1(T) \text{ for all } T \in \mathcal{T}_h\} \subset H^1(\Omega)$$

as well as

$$\mathcal{K}_h := \{\chi \in (V_h)^r \,|\, \chi(x) \in \Sigma, x \in \bar{\Omega}\} \subset \mathcal{K}.$$

Using the construction of the Clément interpolation operator ([20]) it is not difficult to see that for every $\mathbf{u} \in \mathcal{K}$ there exists a sequence $(\hat{\mathbf{u}}_h)_{0<h\leq h_0}$ with $\hat{\mathbf{u}}_h \in \mathcal{K}_h$ such that

$$\hat{\mathbf{u}}_h \to \mathbf{u} \text{ in } H^1(\Omega, \mathbb{R}^r) \text{ as } h \to 0. \tag{3.1}$$

Furthermore, let $(y^h_{obs})_{0<h\leq h_0}$ be a sequence of functions $y^h_{obs} \in \mathcal{O}$ such that

$$y^h_{obs} \to y_{obs} \text{ in } \mathcal{O} \text{ as } h \to 0. \tag{3.2}$$

For $\mathbf{u}_h \in \mathcal{K}_h$ we denote by $y_h = S_h(\mathbf{u}_h) \in V_h$ the solution of

$$\int_\Omega a(\mathbf{u}_h)\nabla y_h \cdot \nabla \chi dx = \int_{\partial\Omega} g_h \chi do \quad \forall \chi \in V_h \tag{3.3}$$

with $\mathcal{M}_{\mathcal{O}}(y_h) = \mathcal{M}_{\mathcal{O}}(y^h_{obs})$. Here $g_h : \partial\Omega \to \mathbb{R}$ is a piecewise linear, continuous approximation to g satisfying

$$\int_{\partial\Omega} g_h do = 0 \text{ and } g_h \to g \text{ in } L^2(\partial\Omega) \text{ as } h \to 0. \tag{3.4}$$

In the same way as in (2.6) one can prove that

$$\|S_h(\mathbf{u}_h)\|_{H^1} \leq c\big(\|g_h\|_{L^2(\partial\Omega)} + \|y^h_{obs}\|_{\mathcal{O}}\big) \leq c \quad \text{uniformly in } \mathbf{u}_h \in \mathcal{K}_h, \tag{3.5}$$

where the constant c is independent of h in view of (3.2) and (3.4).

Lemma 3.1. *Let $(h_k)_{k\in\mathbb{N}}$ be a sequence with $\lim_{k\to\infty} h_k = 0$ and $\mathbf{u}_{h_k} \in \mathcal{K}_{h_k}$ with $\mathbf{u}_{h_k} \to \mathbf{u}$ in $L^1(\Omega, \mathbb{R}^r)$. Then $S_{h_k}(\mathbf{u}_{h_k}) \to S(\mathbf{u})$ in $H^1(\Omega), k \to \infty$.*

Proof. Let $\mathbf{u}_k = \mathbf{u}_{h_k}, y_k = S_{h_k}(\mathbf{u}_k)$ and $y = S(\mathbf{u})$. By passing to a subsequence if necessary we may assume in addition that $\mathbf{u}_k \to \mathbf{u}$ a.e. in Ω. Choose a sequence $\hat{y}_k \in V_{h_k}$ such that $\hat{y}_k \to y$ in $H^1(\Omega)$. Using (2.1) we deduce

$$\begin{aligned}
\|y_k - \hat{y}_k\|_{H^1} &\leq \|y_k - \hat{y}_k - \mathcal{M}_{\mathcal{O}}(y_k - \hat{y}_k)\| + |\Omega|^{\frac{1}{2}}|\mathcal{M}_{\mathcal{O}}(y^{h_k}_{obs} - \hat{y}_k)| + \|\nabla(y_k - \hat{y}_k)\| \\
&\leq c\|\nabla(y_k - \hat{y}_k)\| + |\Omega|^{\frac{1}{2}}\big(|\mathcal{M}_{\mathcal{O}}(y^{h_k}_{obs} - y_{obs})| + |\mathcal{M}_{\mathcal{O}}(y - \hat{y}_k)|\big) \\
&\leq c\|\nabla(y_k - \hat{y}_k)\| + c(\|y^{h_k}_{obs} - y_{obs}\|_{\mathcal{O}} + \|y - \hat{y}_k\|_{H^1}).
\end{aligned} \tag{3.6}$$

In order to estimate the first term we write

$$\begin{aligned}
&\int_\Omega a(\mathbf{u}_k)\nabla(y_k - \hat{y}_k) \cdot \nabla\chi dx \\
&= \int_\Omega a(\mathbf{u}_k)\nabla(y - \hat{y}_k) \cdot \nabla\chi dx + \int_\Omega \big(a(\mathbf{u}) - a(\mathbf{u}_k)\big)\nabla y \cdot \nabla\chi dx + \int_{\partial\Omega} (g_{h_k} - g)\chi do
\end{aligned}$$

for all $\chi \in V_{h_k}$. If we let $\chi = y_k - \hat{y}_k$ and take into account (3.6) we obtain

$$\begin{aligned}
\|y_k - \hat{y}_k\|_{H^1} &\leq c\|y - \hat{y}_k\|_{H^1} + c\Big(\int_\Omega |\mathbf{u}_k - \mathbf{u}|^2|\nabla y|^2 dx\Big)^{\frac{1}{2}} \\
&\quad + c\big(\|g_{h_k} - g\|_{L^2(\partial\Omega)} + \|y^{h_k}_{obs} - y_{obs}\|_{\mathcal{O}}\big) \to 0, k \to \infty
\end{aligned}$$

by (3.4) and (3.2). Here, the second integral is shown to converge to zero in the same way as in the proof of Lemma 2.1. In conclusion, $S_{h_k}(\mathbf{u}_{h_k}) = (y_k - \hat{y}_k) + \hat{y}_k \to y = S(\mathbf{u})$ in $H^1(\Omega)$ and by a standard argument the whole sequence converges. □

Using S_h we define the following approximation $J_{\epsilon,h} : \mathcal{K}_h \to \mathbb{R}$ of J_ϵ:

$$J_{\epsilon,h}(\mathbf{u}_h) := \frac{1}{2}||S_h(\mathbf{u}_h) - y^h_{obs}||^2_{\mathcal{O}} + \sigma \int_\Omega \big(\frac{\varepsilon}{2}|D\mathbf{u}_h|^2 + \frac{1}{2\varepsilon}(1 - |\mathbf{u}_h|^2)\big)dx. \tag{3.7}$$

Theorem 3.2. *There exists $\mathbf{u}_h \in \mathcal{K}_h$ such that $J_{\epsilon,h}(\mathbf{u}_h) = \min_{\mathbf{v}_h \in \mathcal{K}_h} J_{\epsilon,h}(\mathbf{v}_h)$. Every sequence $(\mathbf{u}_{h_k})_{k\in\mathbb{N}}$ with $\lim_{k\to\infty} h_k = 0$ has a subsequence that converges strongly in $H^1(\Omega, \mathbb{R}^r)$ and a.e. in Ω to a minimum of J_ϵ.*

Proof. Since X_h is finite-dimensional, the existence of a minimum of $J_{\epsilon,h}$ is straightforward. Next, let $\mathbf{u}_k \in \mathcal{K}_{h_k}$ be a sequence with $\lim_{k\to\infty} h_k = 0$ and $J_{\epsilon,h_k}(\mathbf{u}_k) = \min_{\mathbf{v}_h \in \mathcal{K}_{h_k}} J_{\epsilon,h_k}(\mathbf{v}_h)$. Since $(\mathbf{u}_k)_{k\in\mathbb{N}}$ is bounded in $H^1(\Omega, \mathbb{R}^r)$, there exists a subsequence, again denoted by $(\mathbf{u}_k)_{k\in\mathbb{N}}$, and $\mathbf{u} \in \mathcal{K}$ such that

$$\mathbf{u}_k \rightharpoonup \mathbf{u} \text{ in } H^1(\Omega, \mathbb{R}^r), \quad \mathbf{u}_k \to \mathbf{u} \text{ in } L^1(\Omega, \mathbb{R}^r) \text{ and a.e. in } \Omega. \tag{3.8}$$

Furthermore, Lemma 3.1 implies that

$$S_{h_k}(\mathbf{u}_k) \to S(\mathbf{u}) \text{ in } H^1(\Omega). \tag{3.9}$$

We claim that $\mathbf{u}$ is a minimum of J_ϵ. To see this, let $\mathbf{v} \in \mathcal{K}$ be arbitrary and $\hat{\mathbf{v}}_k \in \mathcal{K}_{h_k}$ a sequence with $\hat{\mathbf{v}}_k \to \mathbf{v}$ in $H^1(\Omega, \mathbb{R}^r)$, see (3.1). Since $J_{\epsilon,h_k}(\mathbf{u}_k) \le J_{\epsilon,h_k}(\hat{\mathbf{v}}_k)$ we deduce from (3.8), (3.9) and again Lemma 3.1 that

$$J_\epsilon(\mathbf{u}) \le \liminf_{k\to\infty} J_{\epsilon,h_k}(\mathbf{u}_k) \le \limsup_{k\to\infty} J_{\epsilon,h_k}(\mathbf{u}_k) \le \lim_{k\to\infty} J_{\epsilon,h_k}(\hat{\mathbf{v}}_k) = J_\epsilon(\mathbf{v}),$$

so that $J_\epsilon(\mathbf{u}) = \min_{\mathbf{v}\in X} J_\epsilon(\mathbf{v})$. Furthermore, by repeating the above argument with a sequence $\hat{\mathbf{u}}_k \in \mathcal{K}_{h_k}$ such that $\hat{\mathbf{u}}_k \to \mathbf{u}$ in $H^1(\Omega, \mathbb{R}^r)$ we infer in addition that

$$\lim_{k\to\infty} J_{\epsilon,h_k}(\mathbf{u}_k) = J_\epsilon(\mathbf{u}). \tag{3.10}$$

We use this relation to show that $\|D\mathbf{u}_k\|^2 \to \|D\mathbf{u}\|^2$. Namely, let us write

$$\begin{aligned} \frac{\sigma\epsilon}{2}\int_\Omega |D\mathbf{u}_k|^2 dx &= J_{\epsilon,h_k}(\mathbf{u}_k) - \frac{\sigma}{2\epsilon}\int_\Omega (1 - |\mathbf{u}_k|^2)dx - \frac{1}{2}\|S_{h_k}(\mathbf{u}_k) - y^{h_k}_{obs}\|^2_{\mathcal{O}} \\ &\to J_\epsilon(\mathbf{u}) - \frac{\sigma}{2\epsilon}\int_\Omega (1 - |\mathbf{u}|^2)dx - \frac{1}{2}\|S(\mathbf{u}) - y_{obs}\|^2_{\mathcal{O}} = \frac{\sigma\epsilon}{2}\int_\Omega |D\mathbf{u}|^2 dx \end{aligned}$$

in view of (3.10), (3.8), (3.9) and (3.2). Hence $\mathbf{u}_k \to \mathbf{u}$ in $H^1(\Omega, \mathbb{R}^r)$ and the theorem is proved. □

In practice, rather than trying to locate a global minimum of $J_{\epsilon,h}$ one looks for admissible points $\mathbf{u}_h$ that satisfy the necessary first order condition

$$J'_{\epsilon,h}(\mathbf{u}_h)(\mathbf{v}_h - \mathbf{u}_h) \ge 0 \quad \text{for all } \mathbf{v}_h \in \mathcal{K}_h. \tag{3.11}$$

A calculation analogous to (2.11) leads us to the following variational inequality:

$$\sigma \int_\Omega \big(\varepsilon D\mathbf{u}_h \cdot D(\mathbf{v}_h - \mathbf{u}_h) - \frac{1}{\varepsilon}\mathbf{u}_h \cdot (\mathbf{v}_h - \mathbf{u}_h)\big)dx - \int_\Omega (a(\mathbf{v}_h) - a(\mathbf{u}_h))\, \nabla y_h \cdot \nabla p_h dx \geq 0 \quad (3.12)$$

for all $\mathbf{v}_h \in \mathcal{K}_h$, where $y_h = S_h(\mathbf{u}_h)$ and $p_h \in V_h$ with $\mathcal{M}_\mathcal{O}(p_h) = 0$ is the solution of the discrete adjoint problem:

$$\int_\Omega a(\mathbf{u}_h)\nabla p_h \cdot \nabla \chi dx = (y_h - y_{obs}^h, \chi)_\mathcal{O} \quad \forall \chi \in V_h. \tag{3.13}$$

Theorem 3.3. *Let $(\mathbf{u}_{h_k})_{k\in\mathbb{N}}$ be a sequence of solutions of (3.12) with $\lim_{k\to\infty} h_k = 0$. Then there exists a subsequence that converges strongly in $H^1(\Omega, \mathbb{R}^r)$ and a.e. in Ω to a solution $\mathbf{u}$ of (2.11).*

Proof. Let us abbreviate $\mathbf{u}_k = \mathbf{u}_{h_k}, y_k = S_{h_k}(\mathbf{u}_k)$ and denote by $p_k \in V_{h_k}$ the solution of (3.13) with $\mathbf{u}_h = \mathbf{u}_k$ and $y_h = y_k$. Using (3.5) and testing (3.13) with $\chi = p_k$ we infer that

$$\|y_k\|_{H^1} + \|p_k\|_{H^1} \leq c \qquad \text{uniformly in } k \in \mathbb{N}.$$

Next, inserting $\mathbf{v}_h \equiv \frac{1}{r}\sum_{j=1}^r e_j$ into (3.12) we deduce

$$\begin{aligned} \sigma\varepsilon \int_\Omega |D\mathbf{u}_k|^2 dx &\leq \frac{\sigma}{\varepsilon}\int_\Omega |\mathbf{u}_k|^2 dx + \int_\Omega (a(\mathbf{u}_k) - \frac{1}{r}\sum_{i=1}^r a_i)\, \nabla y_k \cdot \nabla p_k dx \\ &\leq \frac{\sigma r}{\varepsilon}|\Omega| + c\|\nabla y_k\|\, \|\nabla p_k\| \leq c. \end{aligned}$$

Hence, there exists a subsequence, again denoted by $(\mathbf{u}_k)_{k\in\mathbb{N}}$, and $\mathbf{u} \in \mathcal{K}$ such that

$$\mathbf{u}_k \rightharpoonup \mathbf{u} \text{ in } H^1(\Omega, \mathbb{R}^r), \quad \mathbf{u}_k \to \mathbf{u} \text{ in } L^1(\Omega, \mathbb{R}^r) \text{ and a.e. in } \Omega. \tag{3.14}$$

Lemma 3.1 implies that

$$y_k = S_{h_k}(\mathbf{u}_k) \to S(\mathbf{u}) =: y \text{ in } H^1(\Omega). \tag{3.15}$$

Let $p \in H^1(\Omega), \mathcal{M}_\mathcal{O}(p) = 0$ be the solution of (2.10). Choose $\hat{p}_k \in V_{h_k}$ with $\mathcal{M}_\mathcal{O}(\hat{p}_k) = 0$ such that $\hat{p}_k \to p$ in $H^1(\Omega)$ and write

$$\begin{aligned} \int_\Omega a(\mathbf{u}_k)\nabla(p_k - \hat{p}_k) \cdot \nabla\chi dx &= \int_\Omega a(\mathbf{u}_k)\nabla(p - \hat{p}_k) \cdot \nabla\chi dx \\ &+ \int_\Omega \big(a(\mathbf{u}) - a(\mathbf{u}_k)\big)\nabla p \cdot \nabla\chi dx + (y_k - y, \chi)_\mathcal{O} - (y_{obs}^{h_k} - y_{obs}, \chi)_\mathcal{O} \end{aligned}$$

for all $\chi \in V_{h_k}$. By choosing $\chi = p_k - \hat{p}_k$ and using (2.1), (3.15) and (3.2) we deduce

$$\|p_k - \hat{p}_k\|_{H^1} \leq c\|\hat{p}_k - p\|_{H^1} + c\Big(\int_\Omega |\mathbf{u}_k - \mathbf{u}|^2 |\nabla p|^2 dx\Big)^{\frac{1}{2}} + c\big(\|y_k - y\|_\mathcal{O} + \|y_{obs}^{h_k} - y_{obs}\|_\mathcal{O}\big) \to 0$$

which implies that $p_k \to p$ in $H^1(\Omega)$.
Let us next show that $\mathbf{u}$ satisfies (2.11). Given $\mathbf{v} \in \mathcal{K}$ there exists a sequence $\hat{\mathbf{v}}_k \in \mathcal{K}_{h_k}$ such that $\hat{\mathbf{v}}_k \to \mathbf{v}$ in $H^1(\Omega, \mathbb{R}^r)$ and a.e. in Ω. Then we have from (3.12)

$$\sigma \int_\Omega \big(\varepsilon D\mathbf{u}_k \cdot D(\hat{\mathbf{v}}_k - \mathbf{u}_k) - \frac{1}{\varepsilon}\mathbf{u}_k \cdot (\hat{\mathbf{v}}_k - \mathbf{u}_k)\big)dx - \int_\Omega (a(\hat{\mathbf{v}}_k) - a(\mathbf{u}_k))\, \nabla y_k \cdot \nabla p_k dx \geq 0. \tag{3.16}$$

In order to examine the second term we write

$$\begin{aligned}\int_\Omega (a(\hat{\mathbf{v}}_k) - a(\mathbf{u}_k))\,\nabla y_k \cdot \nabla p_k dx - \int_\Omega (a(\mathbf{v}) - a(\mathbf{u}))\,\nabla y \cdot \nabla p dx \qquad (3.17)\\ = \int_\Omega (a(\hat{\mathbf{v}}_k) - a(\mathbf{u}_k))[\nabla(y_k - y)\cdot\nabla p_k + \nabla y \cdot \nabla(p_k - p)]dx\\ + \int_\Omega \big((a(\hat{\mathbf{v}}_k) - a(\mathbf{v})) - (a(\mathbf{u}_k) - a(\mathbf{u}))\big)\,\nabla y \cdot \nabla p dx \to 0, k \to \infty\end{aligned}$$

since $y_k \to y, p_k \to p$ in $H^1(\Omega)$ where we used again the dominated convergence theorem for the second integral. By passing to the limit in (3.16) and observing that $\int_\Omega |D\mathbf{u}|^2 dx \le \liminf_{k\to\infty} \int_\Omega |D\mathbf{u}_k|^2 dx$ we infer that $\mathbf{u}$ satisfies (2.11).
Let us finally show that $\mathbf{u}_k \to \mathbf{u}$ in $H^1(\Omega, \mathbb{R}^r)$. Choose a sequence $\hat{\mathbf{u}}_k \in \mathcal{K}_{h_k}$ such that $\hat{\mathbf{u}}_k \to \mathbf{u}$ in $H^1(\Omega, \mathbb{R}^r)$. Inserting $\mathbf{v}_{h_k} = \hat{\mathbf{u}}_k$ into (3.12) we obtain

$$\sigma\epsilon \int_\Omega |D\mathbf{u}_k|^2 dx \le \sigma\epsilon \int_\Omega D\mathbf{u}_k \cdot D\hat{\mathbf{u}}_k dx - \frac{\sigma}{\epsilon}\int_\Omega \mathbf{u}_k \cdot (\hat{\mathbf{u}}_k - \mathbf{u}_k)dx - \int_\Omega \big(a(\hat{\mathbf{u}}_k) - a(\mathbf{u}_k)\big)\,\nabla y_k \cdot \nabla p_k dx$$

so that (3.14) and (3.17) with $\hat{\mathbf{v}}_k = \hat{\mathbf{u}}_k$ imply that

$$\limsup_{k\to\infty} \int_\Omega |D\mathbf{u}_k|^2 dx \le \int_\Omega |D\mathbf{u}|^2 dx.$$

Hence $\int_\Omega |D\mathbf{u}_k|^2 dx \to \int_\Omega |D\mathbf{u}|^2 dx$, so that $D\mathbf{u}_k \to D\mathbf{u}$ in L^2. □

4 An iterative scheme

4.1 Iterative method

Let us consider the following iteration, which can be seen as a time discretization of the parabolic obstacle problem introduced in Remark 2.6. Given $\mathbf{u}_h^n \in \mathcal{K}_h$ let $\mathbf{u}_h^{n+1} \in \mathcal{K}_h$ be the solution of the problem

$$\begin{aligned}\int_\Omega (\mathbf{u}_h^{n+1} - \mathbf{u}_h^n)\cdot(\mathbf{v}_h - \mathbf{u}_h^{n+1})dx - \tau_n \int_\Omega (a(\mathbf{v}_h) - a(\mathbf{u}_h^{n+1}))\,\nabla y_h^n \cdot \nabla p_h^n dx \qquad (4.1)\\ + \tau_n\sigma \int_\Omega \big(\varepsilon D\mathbf{u}_h^{n+1} \cdot D(\mathbf{v}_h - \mathbf{u}_h^{n+1}) - \frac{1}{\varepsilon}\mathbf{u}_h^n \cdot (\mathbf{v}_h - \mathbf{u}_h^{n+1})\big)dx \ge 0 \quad \forall \mathbf{v}_h \in \mathcal{K}_h,\end{aligned}$$

where $\tau_n > 0$, $y_h^n = S_h(\mathbf{u}_h^n)$ and $p_h^n \in V_h$ solves the discrete dual problem

$$\int_\Omega a(\mathbf{u}_h^n)\nabla p_h^n \cdot \nabla \chi dx = (y_h^n - y_{obs}^h, \chi)_{\mathcal{O}} \quad \forall \chi \in V_h \text{ with } \mathcal{M}_{\mathcal{O}}(p_h^n) = 0. \qquad (4.2)$$

Note that $\mathbf{u}_h^{n+1}$ is the unique solution of the convex minimization problem

$$\min_{\mathbf{v}_h \in \mathcal{K}_h} \Big(\frac{1}{2}\|\mathbf{v}_h - \mathbf{u}_h^n\|^2 - \tau_n \int_\Omega a(\mathbf{v}_h)\,\nabla y_h^n \cdot \nabla p_h^n dx + \tau_n\sigma \int_\Omega \big(\frac{\epsilon}{2}|D\mathbf{v}_h|^2 dx - \frac{1}{\epsilon}\mathbf{u}_h^n \cdot \mathbf{v}_h\big)dx\Big).$$

4.2 Convergence of the iterative method

The following result shows that the objective functional decreases in the iteration provided the time steps τ_n satisfy a suitable condition. In order to formulate it we define

$$\hat{a} := \big(\sum_{i=1}^{r} a_i^2\big)^{\frac{1}{2}}, \quad \hat{c} := \inf\Big\{ \frac{\int_\Omega |\nabla\eta|^2 dx}{\|\eta\|_{\mathcal{O}}^2} \,|\, \eta \in H^1(\Omega)\setminus\{0\}, \mathcal{M}_{\mathcal{O}}(\eta) = 0\Big\}. \tag{4.3}$$

Note that $\hat{c} \geq C_p^2 > 0$ in view of (2.1).

Lemma 4.1. *The sequence $(\mathbf{u}_h^n)_{n\in\mathbb{N}_0}$ satisfies*

$$\|\mathbf{u}_h^{n+1} - \mathbf{u}_h^n\|^2 + J_{\epsilon,h}(\mathbf{u}_h^{n+1}) \leq J_{\epsilon,h}(\mathbf{u}_h^n), \quad n \in \mathbb{N}_0,$$

provided that

$$\tau_n \leq \Big(1 + \frac{\hat{a}^2}{a_{min}}\|\nabla y_h^n\|_{L^\infty}\|\nabla p_h^n\|_{L^\infty} + \frac{\hat{a}^2}{a_{min}^2}\frac{1}{2\hat{c}}\|\nabla y_h^n\|_{L^\infty}^2\Big)^{-1}, \qquad n \in \mathbb{N}_0. \tag{4.4}$$

Proof. Inserting $\chi = \mathbf{u}_h^n$ into (4.1) we obtain after some calculations

$$\begin{aligned}
&\frac{1}{\tau_n}\|\mathbf{u}_h^{n+1} - \mathbf{u}_h^n\|^2 + \frac{\sigma\epsilon}{2}\|D(\mathbf{u}_h^{n+1} - \mathbf{u}_h^n)\|^2 + \frac{\sigma}{2\epsilon}\|\mathbf{u}_h^{n+1} - \mathbf{u}_h^n\|^2 \\
&\qquad +\sigma\int_\Omega \big(\frac{\epsilon}{2}|D\mathbf{u}_h^{n+1}|^2 + \frac{1}{2\epsilon}(1 - |\mathbf{u}_h^{n+1}|^2)\big)dx - \sigma\int_\Omega \big(\frac{\epsilon}{2}|D\mathbf{u}_h^n|^2 + \frac{1}{2\epsilon}(1 - |\mathbf{u}_h^n|^2)\big)dx \\
&\leq \int_\Omega a(\mathbf{u}_h^{n+1})\nabla y_h^n \cdot \nabla p_h^n dx - \int_\Omega a(\mathbf{u}_h^n)\nabla y_h^n \cdot \nabla p_h^n dx \equiv: I + II.
\end{aligned} \tag{4.5}$$

Using (3.3) for y_h^n and y_h^{n+1} with test function p_h^n as well as (3.13) we may rewrite II as follows:

$$\begin{aligned}
II &= -\int_\Omega a(\mathbf{u}_h^{n+1})\nabla y_h^{n+1} \cdot \nabla p_h^n dx \\
&= -\int_\Omega a(\mathbf{u}_h^{n+1})\nabla y_h^{n+1} \cdot \nabla p_h^{n+1} dx + \int_\Omega a(\mathbf{u}_h^{n+1})\nabla y_h^{n+1} \cdot \nabla (p_h^{n+1} - p_h^n) dx \\
&= -(y_h^{n+1} - y_{obs}^h, y_h^{n+1})_{\mathcal{O}} + \int_\Omega a(\mathbf{u}_h^{n+1})\nabla y_h^{n+1} \cdot \nabla (p_h^{n+1} - p_h^n) dx \equiv II_1 + II_2.
\end{aligned} \tag{4.6}$$

Using again (3.13) we may write

$$\begin{aligned}
II_1 &= -\frac{1}{2}||y_h^{n+1} - y_{obs}^h||_{\mathcal{O}}^2 + \frac{1}{2}||y_h^n - y_{obs}^h||_{\mathcal{O}}^2 - \frac{1}{2}||y_h^{n+1} - y_h^n||_{\mathcal{O}}^2 - (y_h^{n+1} - y_{obs}^h, y_h^n)_{\mathcal{O}} \\
&= -\frac{1}{2}||y_h^{n+1} - y_{obs}^h||_{\mathcal{O}}^2 + \frac{1}{2}||y_h^n - y_{obs}^h||_{\mathcal{O}}^2 - \frac{1}{2}||y_h^{n+1} - y_h^n||_{\mathcal{O}}^2 \\
&\quad - \int_\Omega a(\mathbf{u}_h^{n+1})\nabla y_h^n \cdot \nabla p_h^{n+1} dx,
\end{aligned}$$

while

$$II_2 = \int_\Omega a(\mathbf{u}_h^n)\nabla y_h^n \cdot \nabla (p_h^{n+1} - p_h^n) dx.$$

Inserting the above identities into (4.6) and combining it with (4.5) we obtain

$$\begin{aligned}
\big(\frac{1}{\tau_n}+\frac{\sigma}{2\epsilon}\big)\|\mathbf{u}_h^{n+1}-\mathbf{u}_h^n\|^2+\frac{\sigma\epsilon}{2}\|D(\mathbf{u}_h^{n+1}-\mathbf{u}_h^n)\|^2+\frac{1}{2}||y_h^{n+1}-y_h^n||_{\mathcal{O}}^2+J_{\epsilon,h}(\mathbf{u}_h^{n+1})\\
\leq\ J_{\epsilon,h}(\mathbf{u}_h^n)+\int_\Omega\big(a(\mathbf{u}_h^n)-a(\mathbf{u}_h^{n+1})\big)\nabla y_h^n\cdot\nabla(p_h^{n+1}-p_h^n)dx\\
\leq\ J_{\epsilon,h}(\mathbf{u}_h^n)+\hat{a}\|\nabla y_h^n\|_{L^\infty}\|\mathbf{u}_h^{n+1}-\mathbf{u}_h^n\|\,\|\nabla(p_h^{n+1}-p_h^n)\|. \qquad (4.7)
\end{aligned}$$

It remains to estimate $\|\nabla(p_h^{n+1}-p_h^n)\|$. To begin, note that

$$\int_\Omega a(\mathbf{u}_h^{n+1})\nabla(p_h^{n+1}-p_h^n)\cdot\nabla\chi dx=\int_\Omega(a(\mathbf{u}_h^n)-a(\mathbf{u}_h^{n+1}))\nabla p_h^n\cdot\nabla\chi dx+(y_h^{n+1}-y_h^n,\chi)_{\mathcal{O}}$$

for all $\chi\in V_h$. Inserting $\chi=p_h^{n+1}-p_h^n$ we deduce that

$$\begin{aligned}
&a_{min}\|\nabla(p_h^{n+1}-p_h^n)\|^2\\
&\quad\leq\ \hat{a}\,\|\nabla p_h^n\|_{L^\infty}\,\|\mathbf{u}_h^{n+1}-\mathbf{u}_h^n\|\,\|\nabla(p_h^{n+1}-p_h^n)\|+\|y_h^{n+1}-y_h^n\|_{\mathcal{O}}\|p_h^{n+1}-p_h^n\|_{\mathcal{O}},
\end{aligned}$$

which implies in view of (4.3)

$$\|\nabla(p_h^{n+1}-p_h^n)\|\leq\frac{\hat{a}}{a_{min}}\|\nabla p_h^n\|_{L^\infty}\,\|\mathbf{u}_h^{n+1}-\mathbf{u}_h^n\|+\frac{1}{\sqrt{\hat{c}}}\frac{1}{a_{min}}\|y_h^{n+1}-y_h^n\|_{\mathcal{O}}.$$

Inserting the above bounds into (4.7) and using (4.4) we infer

$$\begin{aligned}
&\frac{1}{\tau_n}\|\mathbf{u}_h^{n+1}-\mathbf{u}_h^n\|^2+\frac{\sigma\epsilon}{2}\|D(\mathbf{u}_h^{n+1}-\mathbf{u}_h^n)\|^2+\frac{1}{2}||y_h^{n+1}-y_h^n||_{\mathcal{O}}^2+J_{\epsilon,h}(\mathbf{u}_h^{n+1})-J_{\epsilon,h}(\mathbf{u}_h^n)\\
&\leq\ \frac{\hat{a}^2}{a_{min}}\|\nabla y_h^n\|_{L^\infty}\|\nabla p_h^n\|_{L^\infty}\|\mathbf{u}_h^{n+1}-\mathbf{u}_h^n\|^2+\frac{\hat{a}}{a_{min}}\frac{1}{\sqrt{\hat{c}}}\|\nabla y_h^n\|_{L^\infty}\|y_h^{n+1}-y_h^n\|_{\mathcal{O}}\|\mathbf{u}_h^{n+1}-\mathbf{u}_h^n\|\\
&\leq\ \Big(\frac{\hat{a}^2}{a_{min}}\|\nabla y_h^n\|_{L^\infty}\|\nabla p_h^n\|_{L^\infty}+\frac{\hat{a}^2}{a_{min}^2}\frac{1}{2\hat{c}}\|\nabla y_h^n\|_{L^\infty}^2\Big)\|\mathbf{u}_h^{n+1}-\mathbf{u}_h^n\|^2+\frac{1}{2}||y_h^{n+1}-y_h^n||_{\mathcal{O}}^2\\
&\leq\ \big(\frac{1}{\tau_n}-1\big)\|\mathbf{u}_h^{n+1}-\mathbf{u}_h^n\|^2+\frac{1}{2}||y_h^{n+1}-y_h^n||_{\mathcal{O}}^2,
\end{aligned}$$

and the result follows. □

Corollary 4.2. *Let $\mathbf{u}_h^0\in\mathcal{K}_h$. Then the time steps τ_n in (4.1) can be chosen in such a way that $\tau_n\geq\gamma>0, n\in\mathbb{N}$, where γ depends on the data and possibly on h. For this choice the sequence $(\mathbf{u}_h^n)_{n\in\mathbb{N}}$ generated by (4.1) has a subsequence $(\mathbf{u}_h^{n_k})_{k\in\mathbb{N}}$ such that $\mathbf{u}_h^{n_k}\to\mathbf{u}_h$ in $W^{1,\infty}(\Omega,\mathbb{R}^r), k\to\infty$ and $\mathbf{u}_h$ satisfies (3.12).*

Proof. Lemma 4.1 implies that

$$\sum_{n=0}^{\infty}\|\mathbf{u}_h^{n+1}-\mathbf{u}_h^n\|^2\leq J_{\epsilon,h}(\mathbf{u}_h^0),\quad\sup_{n\in\mathbb{N}_0}J_{\epsilon,h}(\mathbf{u}_h^n)\leq J_{\epsilon,h}(\mathbf{u}_h^0),$$

so that $(\mathbf{u}_h^n)_{n\in\mathbb{N}}$ is bounded in $H^1(\Omega,\mathbb{R}^r)$ and

$$\lim_{n\to\infty}\|\mathbf{u}_h^{n+1}-\mathbf{u}_h^n\|=0. \qquad (4.8)$$

In addition we infer from (3.5) and (3.13) that $(y_h^n)_{n\in\mathbb{N}}$ and $(p_h^n)_{n\in\mathbb{N}}$ are also bounded in $H^1(\Omega)$ and hence also in $W^{1,\infty}(\Omega)$ since $\dim V_h < \infty$. In particular, we infer from (4.4) that the time steps τ_n can be chosen to be bounded from below by a positive constant. As a result there exists a subsequence $(\mathbf{u}_h^{n_k}, y_h^{n_k}, p_h^{n_k})_{k\in\mathbb{N}}$ and $(\mathbf{u}_h, y_h, p_h) \in \mathcal{K}_h \times V_h \times V_h$ such that

$$\mathbf{u}_h^{n_k} \to \mathbf{u}_h \text{ in } W^{1,\infty}(\Omega, \mathbb{R}^r), \quad y_h^{n_k} \to y_h, \quad p_h^{n_k} \to p_h \quad \text{ in } W^{1,\infty}(\Omega) \text{ and a.e. in } \Omega.$$

In particular, $y_h = S_h(\mathbf{u}_h)$ and p_h satisfies (3.13). We finally deduce from (4.1)

$$\begin{aligned}\sigma \int_\Omega \big(\varepsilon D\mathbf{u}_h^{n_k+1} \cdot D(\mathbf{v}_h - \mathbf{u}_h^{n_k+1}) - \frac{1}{\varepsilon}\mathbf{u}_h^{n_k} \cdot (\mathbf{v}_h - \mathbf{u}_h^{n_k+1})\big) dx \\ - \int_\Omega (a(\mathbf{v}_h) - a(\mathbf{u}_h^{n_k+1}))\, \nabla y_h^{n_k} \cdot \nabla p_h^{n_k} dx \geq -\frac{1}{\tau_{n_k}} \int_\Omega (\mathbf{u}_h^{n_k+1} - \mathbf{u}_h^{n_k}) \cdot (\mathbf{v}_h - \mathbf{u}_h^{n_k+1}) dx\end{aligned}$$

for all $\mathbf{v}_h \in \mathcal{K}_h$. Recalling (4.8) as well as $\tau_{n_k} \geq \gamma$ we find that $\mathbf{u}_h$ is a solution of (3.12) by passing to the limit $k \to \infty$. □

5 Computational examples

We use a preconditioned biconjugate gradient stabilized solver for the stationary forward problem (3.3) and the adjoint problem (3.13). To solve (4.1) we use the primal-dual active set method presented in [10], where the resulting system of linear equations is solved by applying the direct solver UMFPACK [21].
We set

$$y_{obs} = \tilde{y}_h + \Lambda n(x), \tag{5.1}$$

where $n(x)$ is a random variable with the standard normal zero mean distribution, $\Lambda \in \mathbb{R}$ and $\tilde{y}_h$ is the solution of

$$\int_\Omega a(\tilde{u}_h)\nabla\tilde{y}_h \cdot \nabla\chi dx = \int_{\partial\Omega} g_h\chi do \;\; \forall\chi \in V_h$$

where $\tilde{u}_h$ defines the objective curve.
There is one regularisation parameter σ. When the data is noisy we expect that a suitable size of σ is obtained by balancing the fidelity term with the regularisation term in the objective functional. The size of ε is determined by the need to obtain an accurate approximation of the regularised problem. We note that the thickness of the interfacial layer between bulk regions is proportional to ε. In order to resolve this interfacial layer we need to choose $h \ll \varepsilon$, see [23] for details. Typically reasonable results are obtained with around 8 to 10 elements across the interface. Away from the interface h can be chosen larger and hence adaptivity in space can heavily speed up computations. In fact we use the finite element toolbox Alberta 2.0, see [37], for adaptivity and we implemented the same mesh refinement strategy as in [5], i.e. a fine mesh is constructed for all variables $\mathbf{u}_h^{n+1}, y_h^n$ and p_h^n where $0 < (u_h^n)_i < 1$ for at least one index $i \in \{1, \dots, r\}$ and with a coarser mesh present in the bulk regions where $(u_h^n)_i = 0$ or $(u_h^n)_i = 1$ for all $i \in \{1, \dots, r\}$. In Figure 1 we display a plot of the triangulation of Ω which illustrates the finer mesh within the interface.

In our computations we found it convenient to choose $h_{min} = \frac{1}{256}$ as the minimal diameter, $h_{max} = \frac{1}{64}$ as the maximal diameter of all elements and we set $\tau_n = 0.01/\varepsilon$. The stopping criteria we used to terminate the algorithm was the size of the residual to the first order optimality condition, i.e. $\|(\mathbf{u}_h^{n+1} - \mathbf{u}_h^n)/\tau_n\| \leq 1.0e^{-3}$. For each computation we state the number of iterations, L, required to reach this stopping criteria.
In the case $r = 2$ we have $u_2 = 1 - u_1$ and the vector-valued Allen-Cahn inequality with two order parameters is reduced in the computations to a scalar Allen-Cahn inequality.

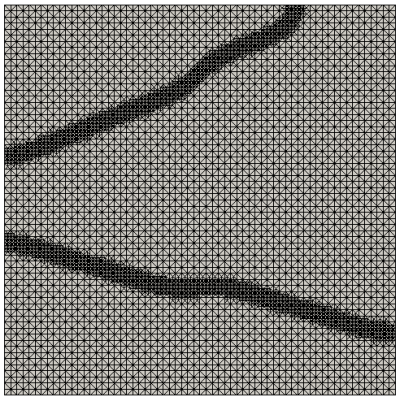

Figure 1: A converged triangulation

5.1 Results with $r = 2$ and $d = 2$

In this section we see how our method compares with the one presented in [31]. In all the computations unless otherwise stated we set $\Omega = (-1, 1)^2$, $J_{fid}(\Gamma) := ||y_\Gamma - y_{obs}||^2_{L^2(\Omega)}$, $\varepsilon = \dfrac{1}{16\pi}$, $a_1 = 3$, $a_2 = 0.5$, $\sigma = 0.0001$, $\Lambda = 0.05$ and

$$g_h(x, y) = \begin{cases} -0.5 & \text{if } x = -1 \text{ or } y = -1 \\ 0.5 & \text{if } x = 1 \text{ or } y = 1. \end{cases}$$

Figure 2 displays the results we obtain when using the same initial curve (a circle of radius 0.6) and objective curve (a 'skinny' ellitpse, $x^2/(0.07)^2 + y^2/(0.5)^2 = 1$) that are used in Section 4.1 of [31]. In this simulation we set $\Lambda = 0$, as in [31]. The left hand plot in Figure 2 displays the initial curve, the centre plot the objective curve and the right hand plot the computed solution $\mathbf{u}_h^n$. The number of iterations required to reach the stopping criteria was $L = 4417$.
Figure 3 takes the same form as Figure 2 except that this time we compare our results with those displayed in Section 4.4 of [31]. The initial curve is again a circle of radius 0.6 while the objective curve consists of two objects

$$\frac{(x + 0.35)^2}{(0.25)^2} + \frac{(y + 0.35)^2}{(0.3)^2} = 1 \quad \text{and} \quad \frac{(x - 0.35)^2}{(0.2)^2} + \frac{(y - 0.35)^2}{(0.2)^2} = 1,$$

as in [31] we set $\Lambda = 0$. The number of iterations required to reach the stopping criteria was $L = 11117$. From this example we see that our phase field model successfully deals with topological change.
In Figure 4 we plot the Residual $:= \|(\mathbf{u}_h^{n+1} - \mathbf{u}_h^n)/\tau_n\|$, $J_{\varepsilon,h}^{fid}(\mathbf{u}_h) := \frac{1}{2}||S_h(\mathbf{u}_h) - y_{obs}^h||_{\mathcal{O}}^2$, $J_{\varepsilon,h}^{reg}(\mathbf{u}_h) := \sigma \int_\Omega \big(\frac{\varepsilon}{2}|D\mathbf{u}_h|^2 + \frac{1}{2\varepsilon}(1 - |\mathbf{u}_h|^2)\big)dx$ and $J_{\varepsilon,h}(\mathbf{u}_h)$ versus iteration number, for the first 2000 iterations, for the computations displayed in Figures 2 and 3. From this figure we see that, in both computations, for the first 50 iterations there is a steep decrease in $J_{\epsilon,h}(\mathbf{u}_h)$ and after that the decrease is much more gradual. We also see that the Residual decreases at a much slower rate than $J_{\epsilon,h}(\mathbf{u}_h)$. In Figure 5 we display two intermediate results from the set-up in Figure 2; the plots display $\mathbf{u}_h^n$ after 150 iterations (left hand plot), after 500 iterations (centre plot) and after 4417 iterations, once the iteration has converged (right hand plot). From this figure we see that after 500 iterations the solution is approximating the shape of the objective curve reasonably well although the curve is not yet defined by a well defined interfacial region.

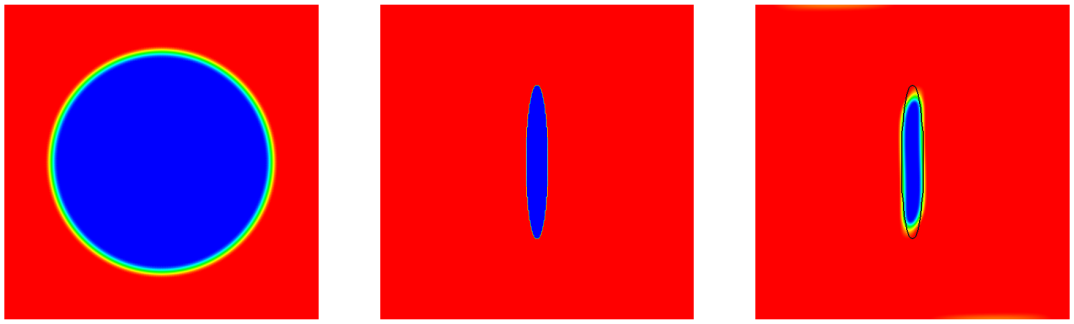

Figure 2: $J_{fid}(\Gamma) := ||y_\Gamma - y_{obs}||_{L^2(\Omega)}^2$, initial curve (left hand plot), objective curve (centre plot), $\mathbf{u}_h^n$ (right hand plot)

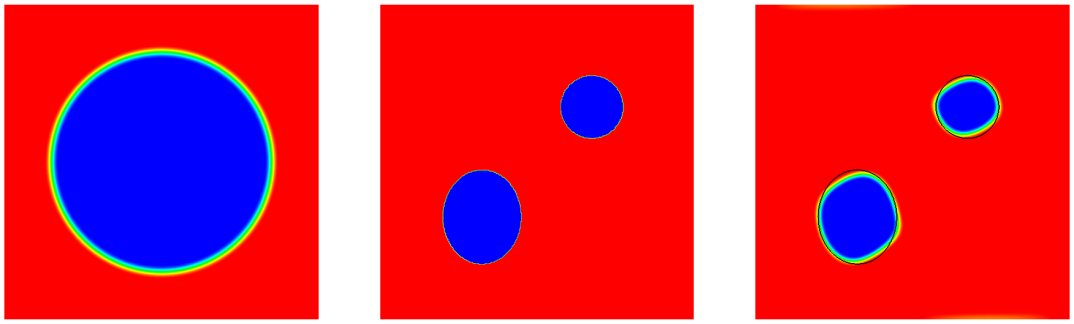

Figure 3: $J_{fid}(\Gamma) := ||y_\Gamma - y_{obs}||_{L^2(\Omega)}^2$, initial curve (left hand plot), objective curve (centre plot), $\mathbf{u}_h^n$ (right hand plot)

In Figure 6 we follow the authors in Section 4.2 of [31] in seeing how noise effects the solution. We take the same initial and objective curves as in Figure 2 and display the solutions obtained with $\Lambda = 0.05$ (left hand plot), $\Lambda = 0.1$ (centre plot) and $\Lambda = 0.2$ (right

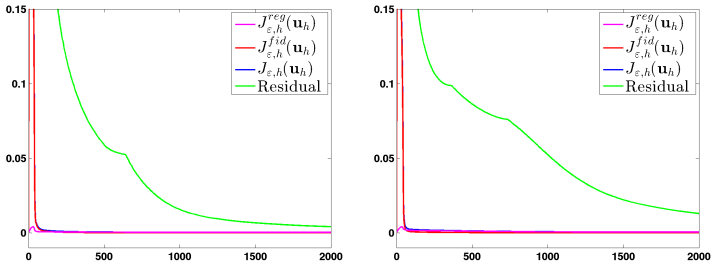

Figure 4: Plot of $J^{fid}_{\varepsilon,h}(\mathbf{u}_h)$, $J^{reg}_{\varepsilon,h}(\mathbf{u}_h)$, $J_{\varepsilon,h}(\mathbf{u}_h)$ and the Residual, versus the number of iterations: results in Figure 2 (left plot), results in Figure 3 (right plot)

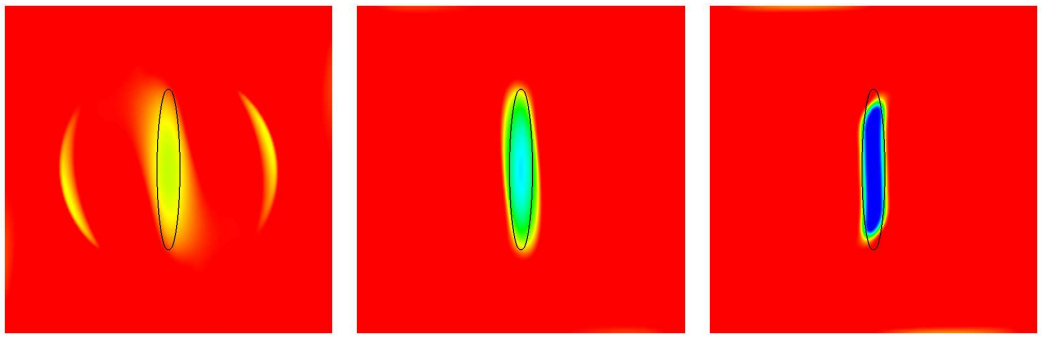

Figure 5: $J_{fid}(\Gamma) := ||y_\Gamma - y_{obs}||^2_{L^2(\Omega)}$, $\mathbf{u}^n_h$ after 150 iterations (left plot), $\mathbf{u}^n_h$ after 500 iterations (centre plot) $\mathbf{u}^n_h$ after 4417 iterations (right plot)

hand plot). The number of iterations required to reach the stopping criteria were $L = 4236$, $L = 4075$ and $L = 8941$ respectively.
In Figure 7 we follow the authors in Section 4.5 of [31] in seeing how the value of the regularisation parameter σ effects the solution. For the initial curve we take a circle of radius 0.7 and for the objective curve we take the ellipse $x^2/(0.5)^2 + y^2/(0.4)^2 = 1$. For the choice $\Lambda = 0.05$ we display the solutions obtained with $\sigma = 0.01$ (top centre) $\sigma = 0.001$ (top right) and $\sigma = 0.0001$ (bottom left) $\sigma = 0.000025$ (bottom centre) $\sigma = 0.0000025$ (bottom right). The number of iterations required to reach the stopping criteria were $L = 3918$, $L = 9183$, $L = 5550$, $L = 8441$ and $L = 21228$ respectively. From this figure we see that $\sigma = 0.001$ and $\sigma = 0.0001$ give the best approximations to the objective curve.
In Figure 8 we plot $J^{fid}_{\epsilon,h}(\mathbf{u}_h)$, $J^{reg}_{\epsilon,h}(\mathbf{u}_h)$, $J_{\epsilon,h}(\mathbf{u}_h)$ and the Residual for the first 4000 iterations, for the computations displayed in Figure 7 with $\sigma = 0.001$, $\sigma = 0.0001$ and $\sigma = 0.000025$. From this figure we see that for $\sigma = 0.001$ the initial decrease in $J_{\epsilon,h}(\mathbf{u}_h)$ is more gradual than for $\sigma = 0.0001$ and $\sigma = 0.000025$.

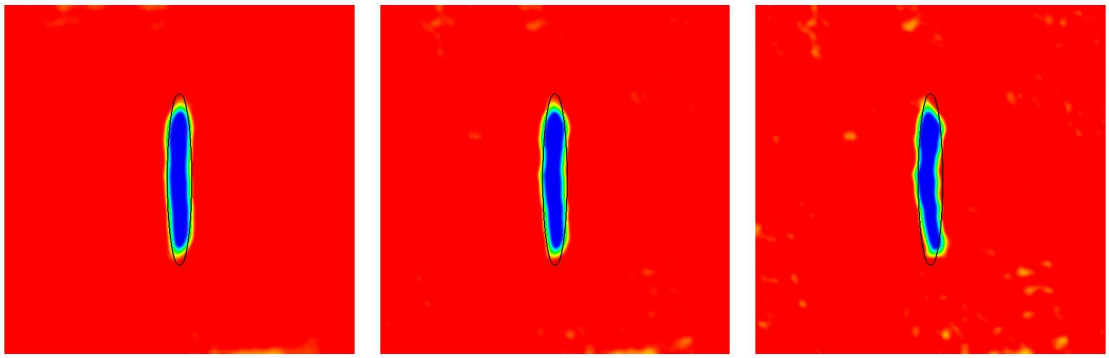

Figure 6: $J_{fid}(\Gamma) := ||y_\Gamma - y_{obs}||^2_{L^2(\Omega)}$, $\mathbf{u}^n_h$ obtained by taking $\Lambda = 0.05$ (left hand plot) $\Lambda = 0.1$ (centre plot) and $\Lambda = 0.2$ (right hand plot)

In Figure 9 we show the effect that the size of $|a_1 - a_2|$ has on the solution $\mathbf{u}^n_h$. We display the objective curve in the left hand plot and in the subsequent plots we display a zoomed in image of the approximate solution, $\mathbf{u}^n_h$, at the end of the simulation obtained from decreasing value of $|a_1 - a_2|$. We take $a_2 = 0.5$ in all plots and $a_1 = 1,\ 3,\ 7$ in the second, third and fourth plots respectively. We see that the approximation to the objective curve improves when $|a_1 - a_2|$ increases. The number of iterations required to reach the stopping criteria were $L = 11891$, $L = 5550$ and $L = 17072$ respectively.
In Figure 10 we show the effect that the choice of $\mathcal{O}$ has on the solution $\mathbf{u}^n_h$. We compare results obtained by taking $J_{fid}(\Gamma) := ||y_\Gamma - y_{obs}||^2_{L^2(\Omega)}$ to results obtained by taking $J_{fid}(\Gamma) := ||y_\Gamma - y_{obs}||^2_{L^2(\partial\Omega)}$. In these simulations we set $\Lambda = 0.02$. We display the objective curve in the left hand plot and the approximate solution $\mathbf{u}^n_h$ at the end of the simulation obtained from $J_{fid}(\Gamma) := ||y_\Gamma - y_{obs}||^2_{L^2(\Omega)}$ (centre plot) and $J_{fid}(\Gamma) := ||y_\Gamma - y_{obs}||^2_{L^2(\partial\Omega)}$ (right plot). From this figure we see that the approximation to the objective curve obtained using $J_{fid}(\Gamma) := ||y_\Gamma - y_{obs}||^2_{L^2(\partial\Omega)}$ is effected more by the noise than the approximation that is obtained using $J_{fid}(\Gamma) := ||y_\Gamma - y_{obs}||^2_{L^2(\Omega)}$. Furthermore using $J_{fid}(\Gamma) := ||y_\Gamma - y_{obs}||^2_{L^2(\Omega)}$ gives

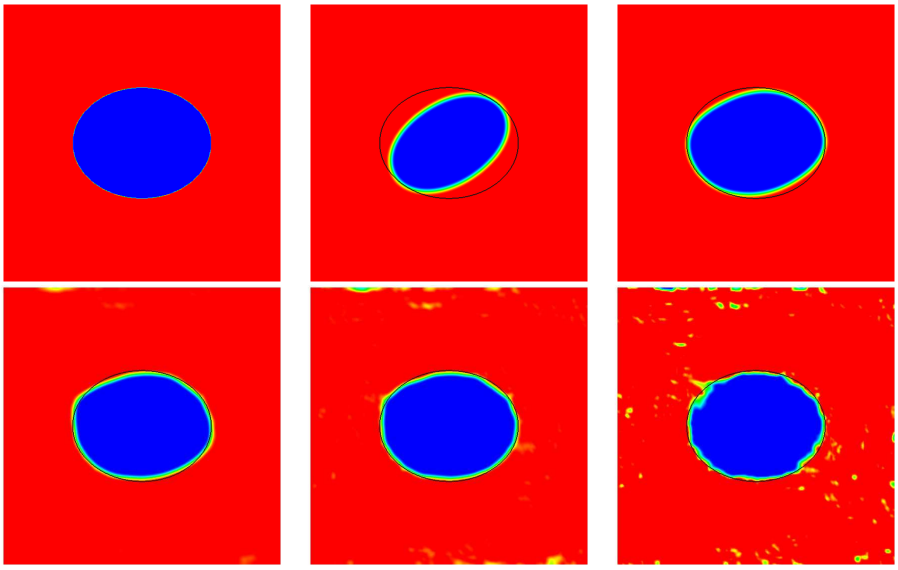

Figure 7: $J_{fid}(\Gamma) := ||y_\Gamma - y_{obs}||^2_{L^2(\Omega)}$, objective curve (top left), $\mathbf{u}_h^n$ obtained by taking $\sigma = 0.01$ (top centre) $\sigma = 0.001$ (top right) and $\sigma = 0.0001$ (bottom left) $\sigma = 0.000025$ (bottom centre) $\sigma = 0.0000025$ (bottom right)

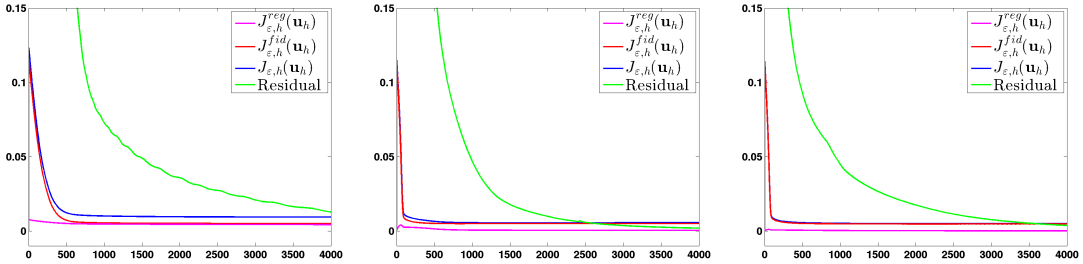

Figure 8: Plot of $J^{fid}_{\varepsilon,h}(\mathbf{u}_h)$, $J^{reg}_{\varepsilon,h}(\mathbf{u}_h)$, $J_{\varepsilon,h}(\mathbf{u}_h)$ and the Residual, versus the number of iterations for the results in Figure 7, $\sigma = 0.001$ (left plot) $\sigma = 0.0001$ (centre plot), $\sigma = 0.000025$ (right plot)

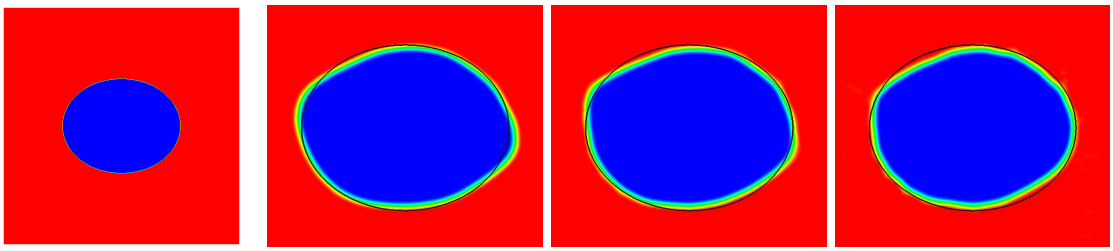

Figure 9: $J_{fid}(\Gamma) := ||y_\Gamma - y_{obs}||^2_{L^2(\Omega)}$, objective curve (first plot), zoomed in plot of $\mathbf{u}_h^n$ obtained by taking $(a_1, a_2) = (1, 0.5)$ (second plot), $(a_1, a_2) = (3, 0.5)$ (third plot) and $(a_1, a_2) = (7, 0.5)$ (fourth plot)

a better approximation to the objective curve than using $J_{fid}(\Gamma) := ||y_\Gamma - y_{obs}||^2_{L^2(\partial\Omega)}$. The number of iterations required to reach the stopping criteria were $L = 16151$ and $L = 18081$ respectively.

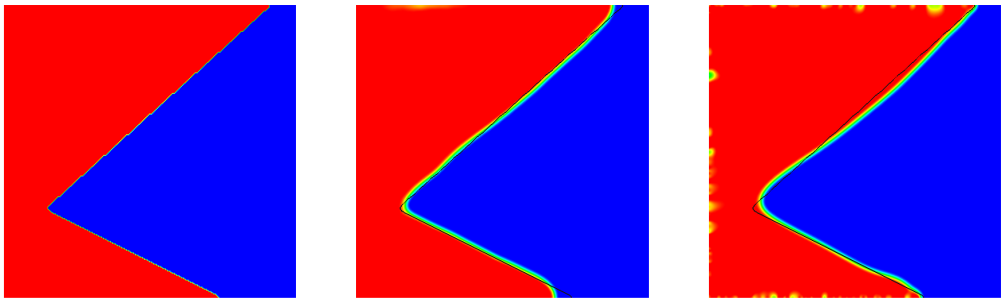

Figure 10: Objective curve (left plot), $\mathbf{u}_h^n$ obtained from $J_{fid}(\Gamma) := ||y_\Gamma - y_{obs}||^2_{L^2(\Omega)}$ (centre plot) and $J_{fid}(\Gamma) := ||y_\Gamma - y_{obs}||^2_{L^2(\partial\Omega)}$ (right plot)

In Figure 11 we display results for three objective curves; we plot the objective curves in the upper row and the solution $\mathbf{u}_h^n$ at the end of the simulation in the lower row. In these simulations we took $\sigma = 0.00001$ and $\Lambda = 0.005$. The number of iterations required to reach the stopping criteria were $L = 12720$, $L = 22296$ and $L = 36036$ respectively. From this figure we see that our method results in good approximations of the objective curves.

5.2 Results with $r = 3$ and $d = 2$

In all the computations in this section we set $\Omega = (-1, 1)^2$, $J_{fid}(\Gamma) := ||y_\Gamma - y_{obs}||^2_{L^2(\Omega)}$, $\varepsilon = \dfrac{1}{8\pi}$, $a_1 = 0.8$, $a_2 = 0.2$, $a_3 = 0.3$, $\sigma = 0.001$, $\Lambda = 0.0$ and

$$g_h(x, y) = \begin{cases} 0 & \text{if } x = \pm 1 \\ -0.5 & \text{if } y = -1 \\ 0.5 & \text{if } y = 1. \end{cases}$$

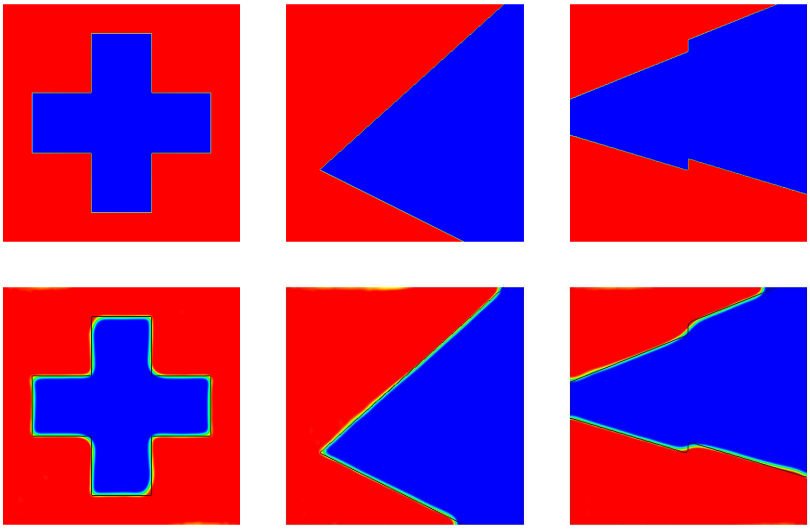

Figure 11: $J_{fid}(\Gamma) := ||y_\Gamma - y_{obs}||^2_{L^2(\Omega)}$, objective curves (upper plots), $\mathbf{u}_h^n$ (lower plots)

In Figure 12 we display results for four objective curves, for each curve we took random t initial data for $\mathbf{u}_h^0$. We plot the objective curves in the upper row and the solution $\mathbf{u}_h^n$ at the end of the simulation in the lower row. The number of iterations required to reach the stopping criteria were $L = 10844$, $L = 33574$, $L = 31113$ and $L = 57373$ respectively.

5.3 Summary of the computational results

The set-up of the computational examples presented in Figures 2, 3, 6 and 7 are taken from examples presented in [31]. The closeness of the approximated curve to the objective curve in the results that we present in Figures 6 and 7 is of a similar order to the results presented in [31]. In the case of Figure 2 the level set method used in [31] yields a better approximation to the skinny ellipse than our phase field model while in the case of Figure 3 our results are a substantial improvement on the ones in [31] as the level set method is unable to deal with the topological change required in this example whereas the phase field model successfully deals with it.

6 Appendix

Theorem 6.1. *Let* $F_\epsilon : X \to \mathbb{R} \cup \{\infty\}$ *be defined by*

$$F_\epsilon(\mathbf{u}) := \begin{cases} \displaystyle\int_\Omega \big(\frac{\epsilon}{2}|D\mathbf{u}|^2 + \frac{1}{2\epsilon}(1 - |\mathbf{u}|^2)\big)dx & , \text{ if } \mathbf{u} \in \mathcal{K}; \\ \infty & , \text{ otherwise.} \end{cases}$$

Then $F_\epsilon \xrightarrow{\Gamma} F$, *where* F *is defined in (2.7).*

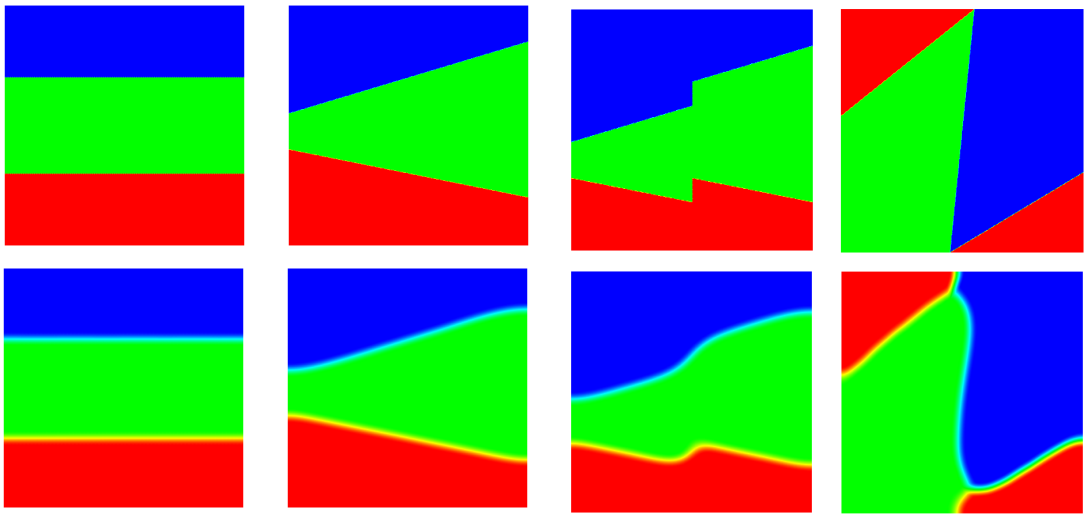

Figure 12: $J_{fid}(\Gamma) := ||y_\Gamma - y_{obs}||^2_{L^2(\Omega)}$, objective curves (upper plots), $\mathbf{u}_h^n$ (lower plots)

Proof. Let us first observe that for $\mathbf{u} \in \mathcal{K}$

$$F_\epsilon(\mathbf{u}) = \sum_{i=1}^r \int_\Omega \big(\frac{\epsilon}{2}|\nabla u_i|^2 + \frac{1}{2\epsilon}(u_i - u_i^2)\big)dx = \sum_{i=1}^r \tilde{F}_\epsilon(u_i),$$

where $\tilde{F}_\epsilon : \tilde{X} := \{v \in L^1(\Omega) \,|\, 0 \le v(x) \le 1 \text{ a.e. in } \Omega\} \to \mathbb{R} \cup \{\infty\}$ is defined by

$$\tilde{F}_\epsilon(v) := \begin{cases} \displaystyle\int_\Omega \big(\frac{\epsilon}{2}|\nabla v|^2 + \frac{1}{2\epsilon}(v - v^2)\big)dx & , \text{ if } v \in H^1(\Omega) \cap \tilde{X}; \\ \infty & , \text{ otherwise.} \end{cases}$$

It is well–known ([33], [1]) that $\tilde{F}_\epsilon \xrightarrow{\Gamma} \tilde{F}$ with

$$\tilde{F}(v) = \begin{cases} \frac{\pi}{8}\mathcal{H}^{d-1}(\partial^*\{v = 1\} \cap \Omega) & , \text{ if } v \in BV(\Omega, \{0,1\}); \\ \infty & , \text{ otherwise.} \end{cases}$$

See [11, 12, 6] and the following development for the calculations leading to the factor $\pi/8$. Let $\mathbf{u} \in X$ and $(\mathbf{u}_{\epsilon_k})_{k\in\mathbb{N}} \subset X$ an arbitrary sequence with $\lim_{k\to\infty} \epsilon_k = 0$ and $\mathbf{u}_{\epsilon_k} \to \mathbf{u}$ in $L^1(\Omega, \mathbb{R}^r)$. Then $(u_{\epsilon_k,i})_{\in\mathbb{N}} \subset \tilde{X}$ and $u_{\epsilon_k,i} \to u_i$ in $L^1(\Omega), i = 1, \dots, r$, so that

$$\liminf_{k\to\infty} F_{\epsilon_k}(\mathbf{u}_{\epsilon_k}) = \liminf_{k\to\infty} \sum_{i=1}^r \tilde{F}_{\epsilon_k}(u_{\epsilon_k,i}) \ge \sum_{i=1}^r \liminf_{k\to\infty} \tilde{F}_{\epsilon_k}(u_{\epsilon_k,i}) \ge \sum_{i=1}^r \tilde{F}(u_i) = F(\mathbf{u})$$

since $\tilde{F}_\epsilon \xrightarrow{\Gamma} \tilde{F}$. It remains to show that for every $\mathbf{u} \in BV(\Omega, \{e_1, \dots, e_r\}) \cap X$ there exists a sequence $(\mathbf{u}_{\epsilon_k})_{k\in\mathbb{N}} \subset \mathcal{K}$ with $\lim_{k\to\infty} \epsilon_k = 0$ such that $\mathbf{u}_{\epsilon_k} \to \mathbf{u}$ in $L^1(\Omega, \mathbb{R}^r)$ and

$$\limsup_{k\to\infty} F_{\epsilon_k}(\mathbf{u}_{\epsilon_k}) \le F(\mathbf{u}). \tag{6.1}$$

We essentially follow the argument in [4]. Because of our particular choice of potential and the absence of volume constraints, the construction can be made more explicit allowing us at the same time to incorporate the condition that $\sum_{i=1}^r u_i(x) = 1$ a.e. in Ω, which isn't considered in [4].
Let $\mathbf{u} \in BV(\Omega, \{e_1, \dots, e_r\}) \cap X$, say $\mathbf{u} = \sum_{i=1}^r \chi_{E_i} e_i$. In view of Lemma 3.1 in [4] we can assume without loss of generality that the E_i are closed polygonal sets satisfying $\mathcal{H}^{d-1}(\partial E_i \cap \partial\Omega) = 0, i = 1, \dots, r$. Lemma 3.3 in [4] implies that there exists $\eta > 0$ such that the functions $h_i : \mathbb{R}^d \to \mathbb{R}$,

$$h_i(x) := \begin{cases} \operatorname{dist}(x, \partial E_i), & x \in \mathbb{R}^d \setminus E_i, \\ -\operatorname{dist}(x, \partial E_i), & x \in E_i, \end{cases}$$

are Lipschitz–continuous on $H_\eta^i := \{x \in \mathbb{R}^d \,|\, |h_i(x)| < \eta\}$ with $|\nabla h_i(x)| = 1$ a.e. in H_η^i. Let us introduce the function $\varphi_\epsilon \in C^1(\mathbb{R})$,

$$\varphi_\epsilon(\tau) := \begin{cases} 0, & \tau \le 0; \\ \frac{1}{2}\big(1 + \sin\big(\frac{\tau}{\epsilon} - \frac{\pi}{2}\big)\big), & 0 < \tau < \epsilon\pi; \\ 1, & \tau \ge \epsilon\pi. \end{cases}$$

Furthermore, we define $\chi_\epsilon : \mathbb{R}^{r-1} \to \mathbb{R}^r$ by

$$[\chi_\epsilon(t)]_i := \begin{cases} 1 - \varphi_\epsilon(t_1) & , i = 1; \\ \varphi_\epsilon(t_1) \cdots \varphi_\epsilon(t_{i-1})(1 - \varphi_\epsilon(t_i)) & , 2 \le i \le r-1; \\ \varphi_\epsilon(t_1) \cdots \varphi_\epsilon(t_{r-1}) & , i = r, \end{cases}$$

where $t = (t_1, \dots, t_{r-1})$. It is not difficult to verify that

$$\chi_\epsilon(t) = \begin{cases} e_1 & , \text{ if } t_1 \le 0; \\ e_i & , \text{ if } t_1 \ge \epsilon\pi, \dots, t_{i-1} \ge \epsilon\pi, t_i \le 0; i = 2, \dots, r-1; \\ e_r & , \text{ if } t_1 \ge \epsilon\pi, \dots, t_{r-1} \ge \epsilon\pi; \end{cases} \tag{6.2}$$

$$0 \le [\chi_\epsilon(t)]_i \le 1,\ i = 1, \dots, r \ \ |D\chi_\epsilon(t)| \le \frac{c}{\epsilon} \text{ a.e. in } \mathbb{R}^{r-1}; \tag{6.3}$$

$$\chi_\epsilon(t) = \frac{1}{2}\big(1 - \sin\big(\frac{t_i}{\epsilon} - \frac{\pi}{2}\big)\big)e_i + \frac{1}{2}\big(1 + \sin\big(\frac{t_i}{\epsilon} - \frac{\pi}{2}\big)\big)e_j, \tag{6.4}$$

$$\text{if } 0 \le t_i \le \epsilon\pi, t_j \le 0, t_k \ge \epsilon\pi, k = 1, \dots, r-1, k \ne i, j \text{ and } i < j.$$

The above function is a particular example of the function χ_ϵ constructed in Lemma 3.2 in [4]. In addition we have

$$\sum_{i=1}^r [\chi_\epsilon(t)]_i = 1, \quad t \in \mathbb{R}^{r-1}.$$

As a consequence, the function $\mathbf{u}_\epsilon(x) := \chi_\epsilon(h_1(x), \dots, h_{r-1}(x)), x \in \Omega$ belongs to $\mathcal{K}$ and satisfies (see p. 79 in [4])

$$\mathbf{u}_\epsilon \to \mathbf{u} \quad \text{ in } L^1(\Omega, \mathbb{R}^r), \epsilon \to 0.$$

In order to analyze $F_\epsilon(\mathbf{u}_\epsilon)$ we introduce as in [4] for $i,j=1,\dots,r$ the sets $\Omega_1^\epsilon := E_1$,

$$\begin{aligned}
\Omega_i^\epsilon &:= \{x\in E_i \,|\, h_j(x) > \epsilon\pi, j=1,\dots,i-1\},\ i=2,\dots,r;\\
\Omega_{ij}^\epsilon &:= \{x\in\Omega \,|\, 0<h_i(x)<\epsilon\pi, h_j(x)<0, h_k(x)>\epsilon\pi, k\neq i,j\} \text{ if } i<j;\\
K_{ij}^\epsilon &:= \{x\in\Omega \,|\, 0\le h_i(x)\le\epsilon\pi, 0\le h_j(x)\le\epsilon\pi\} \text{ if } i<j.
\end{aligned}$$

Then,

$$\Omega\setminus\Big(\bigcup_{i=1}^r\Omega_i^\epsilon\cup\bigcup_{i<j}\Omega_{ij}^\epsilon\Big)\subset\bigcup_{i<j}K_{ij}^\epsilon \tag{6.5}$$

and

$$\mathbf{u}_\epsilon(x)=\begin{cases} e_i, & x\in\Omega_i^\epsilon;\\ \frac{1}{2}\big(1-\sin\big(\frac{h_i(x)}{\epsilon}-\frac{\pi}{2}\big)\big)e_i+\frac{1}{2}\big(1+\sin\big(\frac{h_i(x)}{\epsilon}-\frac{\pi}{2}\big)\big)e_j, & x\in\Omega_{ij}^\epsilon, i<j.\end{cases} \tag{6.6}$$

Abbreviating $F_\epsilon(\mathbf{u},A):=\int_A\big(\frac{\epsilon}{2}|D\mathbf{u}|^2+\frac{1}{2\epsilon}(1-|\mathbf{u}|^2)\big)dx$ we have in view of (6.5) and (6.6)

$$F_\epsilon(\mathbf{u}_\epsilon)\le\sum_{i<j}F_\epsilon(\mathbf{u}_\epsilon,\Omega_{ij}^\epsilon)+\sum_{i<j}F_\epsilon(\mathbf{u}_\epsilon,K_{ij}^\epsilon).$$

It is shown in [4] that $\limsup_{\epsilon\to0}F_\epsilon(\mathbf{u}_\epsilon,K_{ij}^\epsilon)=0$ for $i,j=1,\dots,r, i<j$. Furthermore, observing (6.6) and $|\nabla h_i(x)|=1$ a.e. in Ω_{ij}^ϵ we obtain

$$|D\mathbf{u}_\epsilon(x)|^2=\frac{1}{2\epsilon^2}\cos^2\big(\frac{h_i(x)}{\epsilon}-\frac{\pi}{2}\big),\ \ 1-|\mathbf{u}_\epsilon(x)|^2=\frac{1}{2}\cos^2\big(\frac{h_i(x)}{\epsilon}-\frac{\pi}{2}\big),\quad x\in\Omega_{ij}^\epsilon,$$

so that the coarea formula yields

$$\begin{aligned}
F_\epsilon(\mathbf{u}_\epsilon,\Omega_{ij}^\epsilon)&=\frac{1}{2\epsilon}\int_{\Omega_{ij}^\epsilon}\cos^2\big(\frac{h_i(x)}{\epsilon}-\frac{\pi}{2}\big)dx=\frac{1}{2\epsilon}\int_0^{\epsilon\pi}\cos^2\big(\frac{t}{\epsilon}-\frac{\pi}{2}\big)\,\mathcal{H}^{d-1}(\{h_i=t\}\cap E_j)dt\\
&=\frac{1}{2}\int_{-\frac{\pi}{2}}^{\frac{\pi}{2}}\cos^2(s)\,\mathcal{H}^{d-1}(\{h_i=\epsilon(s+\frac{\pi}{2})\}\cap E_j)ds\to\frac{\pi}{4}\mathcal{H}^{d-1}(\partial E_i\cap\partial E_j\cap\Omega),\epsilon\to0.
\end{aligned}$$

Hence,

$$\limsup_{\epsilon\to0}F_\epsilon(\mathbf{u}_\epsilon)\le\frac{\pi}{4}\sum_{i<j}\mathcal{H}^{d-1}(\partial E_i\cap\partial E_j\cap\Omega)=\frac{\pi}{8}\sum_{i=1}^r\mathcal{H}^{d-1}(\partial E_i\cap\Omega)=F(\mathbf{u}),$$

where we note that $\partial E_i\cap\partial E_j$ is counted twice in the second sum. In conclusion, $F_\epsilon\overset{\Gamma}{\to}F$. □

Corollary 6.2. *Suppose that $(\mathbf{u}_\epsilon)_{\epsilon>0}\subset\mathcal{K}$ is a sequence such that $(F_\epsilon(\mathbf{u}_\epsilon))_{\epsilon>0}$ is bounded. Then there exists a sequence $\epsilon_k\to0$ and $\mathbf{u}\in BV(\Omega,\{e_1,\dots,e_r\})\cap X$ such that $\mathbf{u}_{\epsilon_k}\to\mathbf{u}$ in $L^1(\Omega,\mathbb{R}^r)$.*

Proof. Our assumption yields that $(\tilde{F}_\epsilon(u_{\epsilon,i}))_{\epsilon>0}$ is bounded for $i=1,\dots,r$. It is well–known that this implies that there exists a sequence $\epsilon_k\to0$ and $u_i\in BV(\Omega,\{0,1\})$ such that $u_{\epsilon_k,i}\to u_i$ in $L^1(\Omega)$ and a.e. in $\Omega, i=1,\dots,r$. Clearly, $\mathbf{u}_{\epsilon_k}\to\mathbf{u}=(u_1,\dots,u_r)$ in $L^1(\Omega,\mathbb{R}^r)$, while it also follows that $\sum_{i=1}^r u_i(x)=1$ a.e. in Ω so that $\mathbf{u}\in BV(\Omega,\{e_1,\dots,e_r\})\cap X$. □

Acknowledgements
The third author was supported by the EPSCR grant EP/J016780/1 and the Leverhulme Trust Grant RPG-2014-149.

References

[1] G. Alberti, *Variational models for phase transitions, an approach via Γ–convergence*, in Calculus of variations and partial differential equations (Pisa, 1996), Springer, Berlin, 2000, pp. 95–114.

[2] G. Alessandrini, V. Isakov, and J. Powell, *Local uniqueness in the inverse conductivity problem with one measurement*, Trans. Amer. Math. Soc., **347** (1995), pp. 3031–3041.

[3] H. B. Ameur, M. Burger, and B. Hackl, *Level set methods for geometric inverse problems in linear elasticity*, Inverse Problems, **20** (2004), pp. 673–696.

[4] S. Baldo, *Minimal interface criterion for phase transitions in mixtures of Cahn-Hilliard fluids*, Ann. Inst. H. Poincaré Anal. Non Linéaire, **7** (1990), pp. 67–90.

[5] J. W. Barrett, R. Nürnberg, and V. Styles, *Finite element approximation of a phase field model for void electromigration*, SIAM J. Numer. Anal., **42** (2004), pp. 738–772.

[6] G. Bellettini, M. Paolini, and C. Verdi, *Γ–convergence of discrete approximations to interfaces with prescribed mean curvature*, Atti Accad. Naz. Lincei Cl. Fis. Mat. Natur. Rend. Lincei (9) Mat. Appl., 1 (1990), pp. 317–328.

[7] H. Bellout, A. Friedman, and V. Isakov, *Stability for an inverse problem in potential theory*, Trans. Amer. Math. Soc., **332** (1992), pp. 271–296.

[8] H. Benninghoff and H. Garcke, *Efficient image segmentation and restoration using parametric curve evolution with junctions and topology changes*, SIAM J. Imaging Sciences, **7** (2014), pp. 1451–1483.

[9] L. Blank, M. H. Farshbaf-Shaker, H. Garcke, and V. Styles, *Relating phase field and sharp interface approaches to structural topology optimization,*, Tech. Report Preprint-Nr.: SPP1253-150, DFG priority program 1253 "Optimization with PDEs", 2013.

[10] L. Blank, H. Garcke, L. Sarbu, and V. Styles, *Nonlocal Allen–Cahn systems: analysis and a primal–dual active set method*, IMA J. Numer. Anal., **33** (2013), pp. 1126–1155.

[11] J. F. Blowey and C. M. Elliott, *The Cahn–Hilliard gradient theory for phase separation with non–smooth free energy. I. Mathematical analysis*, European J. Appl. Math., **2** (1991), pp. 233–280.

[12] ——, *Curvature dependent phase boundary motion and parabolic obstacle problems*, in Degenerate Diffusion, Wei-Ming Ni, L. A. Peletier, and J. L. Vasquez, eds., vol. 47 of IMA Vol. Math. Appl., Springer-Verlag, 1993, pp. 19–60.

[13] A. Boyle, A. Adler, and W. R. B. Lionheart, *Shape deformation in two-dimensional electrical impedance tomography*, IEEE Trans. Med. Imaging, **31** (2012), pp. 2185–2193.

[14] A. Braides, Γ-*Convergence for Beginners*, vol. 22 of Oxford Lecture Series in Mathematics and Its Applications, Clarendon Press, 2002.

[15] C. Brett, A. S. Dedner, and C. M. Elliott, *Phase field methods for binary recovery*, LNCSE, Optimization with PDE constraints, ed. R. Hoppe, **101** (2014), pp. 25–63.

[16] M. Burger, *A framework for the construction of level set methods for shape optimization and reconstruction*, Interfaces Free Bound., **5** (2003), pp. 301–329.

[17] T. F. Chan and X.-C. Tai, *Level set and total variation regularization for elliptic inverse problems with discontinuous coefficients*, J. Comput. Phys., **193** (2003), pp. 40–66.

[18] M. Cheney, D. Isaacson, and J. C. Newell, *Electrical impedance tomography*, SIAM review, **41** (1999), pp. 85–101.

[19] C. Clason and K. Kunisch, *Multi-bang control of elliptic systems*, Ann. Inst. H. Poincaré. Anal. Non Linéaire, **31** (2014) 1109–1130.

[20] P. Clément, *Approximation by finite element functions using local regularization*, RAIRO Anal. Numér., R-2 (1975), pp. 77–84.

[21] T. A. Davis, *UMFPACK version 5.2. 0 user guide*, University of Florida, 2007.

[22] A. DeCezaro, A. Leitão, and X.-C. Tai, *On multiple level-set regularization methods for inverse problems*, Inverse Problems, **25** (2009), pp. 035004, 22.

[23] K. Deckelnick, G. Dziuk, and C. M. Elliott, *Computation of geometric partial differential equations and mean curvature flow*, Acta Numerica, **14** (2005), pp. 139–232.

[24] O. Dorn, E. L. Miller, and C. M. Rappaport, *A shape reconstruction method for electromagnetic tomography using adjoint fields and level sets*, Inverse Problems, **16** (2000), p. 1119.

[25] O. Dorn and R. Villegas, *History matching of petroleum reservoirs using a level set technique*, Inverse Problems, **24** (2008), p. 035015.

[26] B. Hackl, *Methods for reliable topology changes for perimeter-regularized geometric inverse problems*, SIAM J Numer Anal, **45** (2007), pp. 2201–2227.

[27] J. Hegemann, A. Cantarero, C. L. Richardson, and J. M. Teran, *An explicit update scheme for inverse parameter and interface estimation of piecewise constant coefficients in linear elliptic pdes*, SIAM J. Sci. Comput., **35** (2013), pp. A1098–A1119.

[28] F. Hettlich and W. Rundell, *The determination of a discontinuity in a conductivity from a single boundary measurement*, Inverse Problems, **14** (1998), pp. 67–82.

[29] M. A. Iglesias, K. Lin, and A. M. Stuart, *Well-posed Bayesian geometric inverse problems arising in subsurface flow*, Inverse Problems, **30** (2014), 114001.

[30] M. A. Iglesias and D. McLaughlin, *Level-set techniques for facies identification in reservoir modeling*, Inverse Problems, **27** (2011), p. 035008.

[31] K. Ito, K. Kunisch, and Z. Li, *Level-set function approach to an inverse interface problem*, Inverse Problems, **17** (2001), pp. 1225–1242.

[32] V. Kolehmainen, S. R. Arridge, W. R. B. Lionheart, M. Vauhkonen, and J. P. Kaipio, *Recovery of region boundaries of piecewise constant coefficients of an elliptic PDE from boundary data*, Inverse Problems, **15** (1999), pp. 1375–1391.

[33] L. Modica, *The gradient theory of phase transitions and the minimal interface criterion*, Arch. Rational Mech. Anal., **98** (1987), pp. 123–142.

[34] D. Mumford and J. Shah, *Optimal approximations by piecewise smooth functions and associated variational problems*, Communications on Pure and Applied Mathematics, **42** (1989), pp. 577–685.

[35] L. K. Nielsen, X.-C. Tai, S. I. Aanonsen, and M. Espedal, *A binary level set model for elliptic inverse problems with discontinuous coefficients*, Int. J. Numer. Anal. Model., **4** (2007), pp. 74–99.

[36] F. Santosa, *A level-set approach for inverse problems involving obstacles*, ESAIM Contrôle Optim. Calc. Var., 1 (1995/96), pp. 17–33.

[37] A. Schmidt and K. G. Siebert, *Design of adaptive finite element software: The finite element toolbox ALBERTA*, vol. 42 of Lecture notes in computational science and engineering, Springer, 2005.

[38] X.-C. Tai and H. Li, *A piecewise constant level set method for elliptic inverse problems*, Appl. Numer. Math., **57** (2007), pp. 686–696.

[39] A. Tsai, A. Yezzi, and A.S. Willsky, *Curve evolution implementation of the Mumford–Shah functional for image segmentation, denoising, interpolation, and magnification*, IEEE Trans. Image Processing, **10** (2001).

[40] K. van den Doel, U. M. Ascher, and A. Leitão, *Multiple level sets for piecewise constant surface reconstruction in highly ill-posed problems*, J. Sci. Comput., **43** (2010), pp. 44–66.